Energetic Nitrogen Ions within the Inner Magnetosphere of Saturn

By

E.C. Sittler Jr.[1], R.E. Johnson,[2] H.T. Smith[2], J.D. Richardson[3], S. Jurac[3], M. Moore[1], J.F. Cooper[4], B. H. Mauk[5], M. Michael[2], C. Paranicas[5], T. P. Armstrong[6], and B. Tsurutani[7]

1. **NASA/Goddard Space Flight Center/Greenbelt, MD**
2. **University of Virginia/Charlottesville, VA**
3. **Massachusetts Institute of Technology/Cambridge, MA**
4. **Raytheon Technical Services Company LLC, NASA Goddard Space Flight Center, Greenbelt, MD**
5. **Applied Physics Laboratory/Laurel, MD**
6. **Fundamental Technology, Lawrence, KS**
7. **Jet Propulsion Laboratory, Pasadena, CA**

ABSTRACT

We investigate the importance of nitrogen ions within Saturn's magnetosphere and their contribution to the energetic charged particle population within Saturn's inner magnetosphere. This study is based on the Voyager observations of Saturn's magnetosphere and Cassini observations. The latter have shown that water group ions dominate both the plasma [Young et al., 2005; Sittler et al., 2005a] and energetic particle populations [Krimigis et al., 2005], but that nitrogen ions over a broad range of energies were observed at ~ 5% abundance level [Smith et al., 2005; Krimigis et al., 2005]. In the outer magnetosphere methane ions were predicted to be an important pickup ion at Titan [Sittler et al., 2004a, 2005b] and were detected at significant levels in the outer magnetosphere [Crary et al., 2005] and at Titan [Hartle et al., 2006]. O^+ ions were found to be the dominant heavy ion in the outer magnetosphere, ~ 60%, with methane ions being ~ 30% of the heavy ions and N^+ a few percent [Crary et al., 2005]. The two major sources of nitrogen ions within Saturn's magnetosphere are Titan's atmosphere and primordial nitrogen trapped in the icy crust of Saturn's moons and its ring particles deep within the magnetosphere. It is important to understand the source, transport and sinks of nitrogen in order to determine whether they have a primordial origin or are from Titan's atmosphere. The energetic component is important, since it can come from Titan, be implanted into the surfaces of the icy moons and reappear at plasma energies via sputtering obfuscating the ultimate source. As we will show, such implantation of nitrogen ions can produce interesting chemistry within the ice of Saturn's moons. The emphasis will be on the nitrogen, but the oxygen and other water group ions are also considered. We argue that neutral clouds of heavy atoms and molecules within Saturn's outer magnetosphere may be the dominant source of energetic heavy ions observed within the inner magnetosphere. Pickup heavy ions in the outer magnetosphere have

energies ~ 1-4 keV when born. If they diffuse radially inward, while conserving the first and second adiabatic invariants, they can have energies greater than several hundred keV inside of Dione's L shell. We will show how observations relate to the various sources and acceleration processes such as ionization, collisions, wave-particle interactions and radial diffusion.

1.0 **INTRODUCTION**

Data from Pioneer 11 and Voyager flybys of Saturn and Cassini observations during Saturn Orbit Insertion (SOI) show that the magnetosphere contains a significant population of trapped, energetic (>10keV) heavy ions. The heavy ions are of interest as they are likely to come from sources orbiting in Saturn's magnetosphere and act as agents for chemical change and erosion via surface sputtering, implantation, and radiolysis of objects embedded in Saturn's magnetosphere. The composition of these energetic heavy ions, based on Cassini observations, is dominated by water with a small nitrogen contribution. Saturn's atmosphere and the solar wind are sources of light ions. Titan is a source of hydrogen, nitrogen and methane [Sittler et al., 2005b; Crary et al., 2005; Hartle et al., 2006], while the icy moons and rings are sources of water molecules and possibly nitrogen [Sittler et al., 2004b; Young et al., 2005; Smith et al., 2005; Sittler et al., 2005a]. On dissociation and ionization this results in a rotating oxygen and water group ion plasma in the inner magnetosphere, and oxygen-methane plasma in the outer magnetosphere with a minor contribution of nitrogen throughout. As in the Jovian system O^+ ions within the inner magnetosphere can go through a charge exchange cycle, propagate freely outward as neutrals, become ionized again by photo-ionization and become a source of energetic heavy ions via inward diffusion and acceleration. This mechanism could make the observed energetic O^+ and water group ions within Saturn's inner magnetosphere. Eviatar et al. [1983], originally suggested that charge exchange reactions between co-rotating O^+ ions and atomic hydrogen at the outer edge of the A-ring ($r \sim 2.25\ R_S$), might produce a source of neutral oxygen within Saturn's outer magnetosphere ($11.2 < r < 29.1\ R_S$) with a source strength as large as $S_O \sim 1.4 \times 10^{26}$ atoms/s. Johnson et al. [1989] also suggested recycling of water products by low energy orbiting collisions inside of the orbit of Enceladus. More recently, Johnson et al. [2005] have shown that low speed charge exchange reactions are expected to be important within Saturn's inner magnetosphere so that the ejected neutrals will be gravitationally bound to Saturn and form neutral clouds of oxygen and water molecules within Saturn's outer magnetosphere. This mechanism has been referred to as charge exchange transport. This source of oxygen and water molecules evidently exceeds our estimate of the nitrogen torus $S_N \sim 4.5 \times 10^{25}$ atoms/s by more than an order of magnitude and explains the observed domination of oxygen ions relative to nitrogen ions within the outer magnetosphere [Johnson et al., 2005]. The ionization of the heavy neutral gas forming this giant cloud around Saturn will form an outer torus of hot keV heavy ions around Saturn. A fraction of these ions are expected to diffuse radially inward and become a source of energetic heavy ions for the inner magnetosphere. This inward transport of hot plasma has been identified as injection events as observed by the Cassini plasma instrument [Burch et al., 2005]. Due to the complexity of the composition within Saturn's magnetosphere we will refer to the more dominant O^+, water group ions (W^+) and

methane ions (CH_4^+) and their fragments (i.e., CH_3^+, CH_2^+, CH^+, C^+), as simply O^+ unless otherwise stated.

The Voyager LECP instrument could not discriminate between O^+ and N^+, but the recent Cassini observations have shown O^+ and water group ions to dominate the energetic particle flux of heavy ions [Krimigis et al., 2005]. Some had suggested that Titan, and thus N^+, was the dominant source [Barbosa, 1987], but others had advocated an O^+ source derived from water products ejected from the surfaces of the icy satellites and E-ring grains via sputtering [Johnson et al., 1989]. Recent examination of Voyager LECP data had suggested far fewer energetic heavy ions than originally thought. If true this would lower sputtering rates than were assumed earlier [Jurac et al. 2001; Paranicas et al, 2004]. But, Cassini observations have clearly shown that energetic heavy ions are important. It is also clear that the thermal plasma is dominated by water products, with a minor N^+ component. Therefore, heavy ions probably dominate the sputtering rates for the icy satellites as originally thought.

We first review the analysis of the Titan source rate and then describe the results of the most recent models for loss of atmosphere from Titan and the resultant formation of a neutral and plasma torus. We then re-examine the Voyager data and re-analyze the various sources of plasma for Saturn's magnetosphere. A brief examination of the loss processes follows, which will appear in a separate paper [Sittler et al., 2006, manuscript in preparation]. We then examine the situation at Dione as indicated by Voyager and consider the effect of energetic nitrogen on the surface of Dione, in the context of energetic oxygen dominating the surface chemistry. The surface radiolysis is shown to be dominated by the magnetospheric electron population.

1.1 Titan's Neutral Torus: Review of Models

Strobel and Shemansky [1982] studying Voyager 1 UVS data at Titan [see Broadfoot et al., 1981] identified EUV emissions consistent with electron impact dissociation of N_2 at Titan's exobase and the corresponding ejection of energetic nitrogen atoms from Titan. They suggested that these nitrogen atoms would form a giant nitrogen torus around Saturn with a source strength $S_N \sim 3 \times 10^{26}$ atoms/sec. This was followed by papers based on Voyager plasma observations by Eviatar et al. [1983] and Eviatar and Podolak [1983], which suggested an atomic nitrogen source strength of $S_N \sim 7.5 \times 10^{25}$ atoms/sec. Further support of this result was offered by Hunten et al. [1984] who showed that Titan should be an important source of neutral atoms and molecules within Saturn's magnetosphere, while Hunten [1982] and Johnson [1994] showed that nonthermal mechanisms were important for atmospheric escape from Titan. Barbosa [1987] estimated the dimensions of this atomic nitrogen torus based on ejection speeds at the exobase of 1-2 km/sec and on a source strength of $S_N \sim 6 \times 10^{26}$ atoms/sec. He also estimated that the torus would have radial extent between 8 R_S and 25 R_S and thickness between 8 R_S and 16 R_S depending on the assumed ejection velocities and an average nitrogen density of 6 atoms/cm^3. He then argued that the atomic nitrogen atoms would be ionized with a time scale $\tau \sim 3 \times 10^7$ sec and that the nitrogen N^+ ions would have pickup energies of several keV forming a suprathermal component for the ambient ions as observed by the Voyager

plasma instrument [Lazarus and McNutt, 1983]. It was argued that these suprathermal pickup nitrogen ions would then accelerate thermal electrons to energies ~ 1 keV via wave-particle interactions by lower hybrid waves [Barbosa, 1986]. This prediction was supported by Voyager plasma electron observations [Sittler et al., 1983]. Barbosa [1987] further argued that the magnetometer results reported by Connerney et al. [1983] with Z3 internal field and ring current supported the mapping of field lines within the Titan torus to around 80° north latitude at Saturn where the aurora was observed [Broadfoot et al., 1981; Sandel et al., 1982]. The pickup energy of the suprathermal nitrogen ions within the Titan torus could provide a power level ~ 2 x 10^{11} watts for the precipitating keV electrons that would power the aurora as required by the Voyager UVS observations [Sandel and Broadfoot, 1981]. Sandel and Broadfoot [1981] also found the auroral emissions were consistent with Saturn's kilometric radiation [Warwick et al., 1981] for which the UV aurora was brightest at a sub-solar longitude ~ 100°. The importance of an internal energy source for producing the aurora and SKR is also supported by the theoretical considerations by Curtis et al. [1986] and more recently by Sittler et al. [2006], who considered the centrifugally driven flute instability.

The source strength of the ejected nitrogen atoms was revised downward by Strobel et al. [1992] from their original analysis [Strobel and Shemansky, 1982] to $S_N < 10^{25}$ atoms/sec, using revised cross-sections and showing that most of the EUV emission observed by Voyager came from solar UV and photoelectrons and not by magnetospheric electron impact dissociation of N_2 gas. The main reason for this decrease was the placement [see also Hartle et al., 1982] of the ionopause at R_i ~ 4400 km with the exobase being located at R_{exo} ~ 4000 km. Because the scale height (~ 70 km) is much less than 400 km, the magnetospheric plasma electrons in this model did not have direct access to Titan's atmosphere and could only reach the exobase via curvature drift. Furthermore, because the Alfven conductance is much less than the ionospheric conductance, the magnetospheric plasma could not penetrate the ionopause and reach the exobase or lower altitudes. The key to the true estimate of the source term is the actual location of the ionopause relative to the exobase.

Ip [1992] did a more in depth analysis of the magnetospheric interaction issues regarding the ejection of fast neutrals and formation of a Titan nitrogen torus. In this model he estimated an energy spectrum of the fast nitrogen atoms and developed a Monte Carlo description of the torus, which included the collisional transport of the atomic fragments through Titan's atmosphere. Ip stated that the primary reactions responsible for the ejection of fast neutrals (N^*) were the following:

$$N_2 + e \rightarrow N_2^+ + 2e \quad (1)$$

$$N_2 + e \rightarrow N^+ + N^* + 2e \quad (2)$$

$$N_2 + e \rightarrow N^* + N^* + e \quad (3)$$

Reaction 1 is then followed by electron dissociative recombination of N_2^+ to produce fast N*. He then argued, using his earlier ionospheric model [Ip, 1990], that the dominant ion

within the ionosphere could be N_2^+ with $N_i \sim 3x10^3$ ions/cm^3 and that this peak density could be located near the exobase at $R_{exo} \sim 4000$ km within a scale height H ~ 70 km; this ionopause height is considerably less than that estimated by Strobel et al. [1992]. Ip's model therefore allowed magnetospheric plasma electrons to have access to Titan's upper atmosphere. Below the exobase collisions are important, so that it will be more difficult for fast neutrals from Eqs. 1-3 to escape from Titan. The electron dissociation of N_2^+ can produce N atoms with energies greater than the escape energy (0.3eV) due to the excess energy released, $\Delta E = 1.75$ eV. From this mechanism alone the source term is $S_N \sim 2x10^{25}$ atoms/sec. For reaction 2 the launch energies for fast neutrals vary between 0.25 eV and 4 eV. Ip [1992] argued that the bite-out in magnetospheric electrons for E>700 eV reported by Hartle et al. [1982], implies that magnetospheric electrons, via curvature drift, penetrate down to the exobase. He then said that reaction 3 will tend to dominate with $\Delta E \approx 0.35$ eV [see McElroy et al. [1972] and Rees [1989]], so that the ejection energies are low. Ip [1992] noted that Barbosa and Eviatar [1986] and Barbosa [1987] favor reaction 3. Ip [1992] points out that the vertical distributions of the magnetospheric plasma, ionospheric plasma and extended neutral atmosphere of Titan are complex in the vicinity of the exobase and that modeling the ejection of fast neutrals is very uncertain. The energy spectrum of fast neutrals is also very uncertain. Ip [1992] used a source term $S_N \sim 7x10^{25}$ atoms/sec and had peak densities between [N] = 3-20 atoms/cm^3 at Titan's L shell for which he primarily used reaction 2. On adding reaction 3 he found an additional peak density of 5-50 atoms/cm^3 at Titan's L shell. Since charge exchange is the dominant loss mechanism, the lower range of neutral densities applies when one uses the shorter N atom lifetime $\tau \sim 3x10^7$ seconds from interaction with ambient magnetospheric N^+ within Titan's nitrogen torus versus a longer lifetime $\tau \sim 3x10^8$ seconds when the ambient ion is O^+. Since O^+/CH_4^+ ions dominate over N^+ ions in the outer magnetosphere [Crary et al., 2005; Hartle et al., 2005], the longer lifetime applies and the N atom densities would be ~ 40 atoms/cm^3. Here, we note that although the charge exchange process does not change the number of ions in the plasma, it does replace a more abundant cold ambient ion with a hot keV heavy ion such as O^+/N^+. The net result is an increase in the plasma energy density and increase in plasma $\beta \sim 11$ [see Neubauer et al., 1984].

Lammer and Bauer [1993] included the impact of magnetospheric heavy ions onto Titan's upper atmosphere and the corresponding sputtering of fast neutrals such as N and N_2. They predicted that sputtering was a more important mechanism than magnetospheric electron impact dissociation of N_2 and photo-dissociation of N_2 for production of fast neutrals at the exobase. See Johnson [1994] for details about the physics of atmospheric sputtering. This mechanism can be important since the ion gyro-radii are much larger than an atmospheric scale height and the ions have direct access to the atmosphere below the exobase even if the ionopause is 400 km above the exobase in height. However, the model by Lammer and Bauer [1993] ignored collisions below the exobase, and thereby over-estimated the magnitude of the source of fast neutrals for the Titan nitrogen torus.

Shematovich et al. [2001] showed the sputtering estimate by Lammer and Bauer [1993] was much too large. The net source rate is $S_N \sim 3x10^{25}$ atoms/sec considering atmospheric sputtering by the rotating plasma ions and magnetospheric electron impact dissociation and photo-dissociation contributions. Sputtering can produce energetic

neutrals with mean escape energies ~ 2.2 eV to 7.0 eV, which is significantly greater than that produced by magnetospheric electron impact dissociation of N_2 (i.e., ΔE ~ 0.25 eV to 4.0 eV) or photo-dissociation of N_2 (i.e.,ΔE ~1.43 eV). However, they found that the dissociation of N_2 by solar EUV photons and corresponding flux of photoelectrons dominated over the sputtering mechanism. In these estimates the slowing of the plasma and the pick-up of heavy ions were ignored. Using estimates of these effects, Shematovich et al. [2003] found that sputtering is competitive with photo-dissociation for producing escaping N atoms and dominates the production of escaping N_2 molecules. A combined source strength $S_N \sim 3.6x10^{25}$ N/sec was given. More recently Michael et al. [2005] estimated a source $S_N \sim 4.6x10^{25}$ N/sec. These calculations used the upstream plasma properties defined by the hybrid model of the Titan interaction with Saturn's magnetosphere by Brecht et al. [2000]. This provided a more realistic description of the interaction. The variation in source strength as described above, depending on the model used, underscores the difficulty in estimating the flux of escaping fast nitrogen atoms and molecules from Titan's upper atmosphere and their corresponding contribution to Titan's nitrogen torus. Therefore, we assign an order of magnitude uncertainty to S_N.

Cravens et al. [1997], using chemistry initiated by photo and electron impact ionization and dissociation without sputtering estimated an upper limit for the source term $S_N \sim 2.5x10^{25}$ atoms/sec of fast N atoms for the Titan nitrogen torus. They also considered other fast atoms and molecules ejected by this mechanism. Here the chemistry would have a carbon contribution. The various estimates of the nitrogen torus source strength are summarized in Table 1.

Table 1. Titan Neutral Torus

- Strobel and Shemansky, 1982 — $S_N \sim 3x10^{26}$ N/s
- Eviatar and Podolak, 1983 — $S_N \sim 7.5x10^{25}$ N/s
- Barbosa, 1987 — $S_N \sim 6x10^{26}$ N/s
- Strobel et al., 1992 — $S_N < 10^{25}$ N/s
- Ip, 1992 — $S_N \sim 7x10^{25}$ N/s
- Lammer and Bauer, 1993 — $S_N > 10^{26}$ N/s
- Cravens et al., 1997 — $S_N \sim 2.5x10^{25}$ N/s
- Shematovich et al., 2001 — $S_N \sim 3x10^{25}$ N/s
- Shematovich et al., 2003 — $S_N \sim 3.6x10^{25}$ N/s
- Michael et al., 2005 — $S_N \sim 4.6x10^{25}$ N/s
- We have developed a Monte Carlo Model of the nitrogen torus using $S_N \sim 4.5x10^{25}$ N/s, U = 0.3 eV and v = 1 km/s launch speed.

In addition to the atomic nitrogen torus discussed above, there is the well known atomic hydrogen torus originally detected by McDonough and Brice [1973] with mean density [H] ~ 20 atoms/cm^3 [see also Broadfoot et al., 1981]. Shemansky and Hall [1992] have shown that this hydrogen cloud permeates the Saturn system and is not confined to a torus centered on Titan's orbital position. The hydrogen torus is similar in extent to the nitrogen torus with the added advantage that it has been observed via the strong Lyman alpha emissions, while the nitrogen torus has not yet been detected. The UVIS instrument

on Cassini [Esposito et al., 2004] has not yet detected this nitrogen torus [D. E. Shemansky, private communication, 2004]. The pickup energies for the H^+ ions are less than 100 eV and cannot explain the observation of keV ions in the outer magnetosphere as reported by Lazarus and McNutt [1983] and Eviatar et al. [1983] or provide the necessary power for the observed Saturn aurora [Sandel and Broadfoot, 1981]. The Cassini Plasma Spectrometer (CAPS) [Young et al., 2004], will be able to measure these pickup ions and their composition throughout Saturn's magnetosphere.

1.2 Solar Wind and Nitrogen Torus as Source of Hot Plasma

A potentially important source of keV ions within Saturn's outer magnetosphere is the solar wind mainly protons and alpha particles. These ions already have keV energies and can be further energized within Saturn's magnetosphere where the cross-tail potential is ~ 50 kV. Note, that the solar wind was originally considered by Sandel and Broadfoot [1981] as the energy source for Saturn's aurora. The solar wind ions can leak into Saturn's magnetosphere via reconnection at the low latitude boundary layer [Tsurutani et al., 2001, 2003], polar cusp and magnetopause and sub-storms at Saturn might play in this process [Cowley et al., 2005]. Tsurutani et al. [2003] presented evidence for the Earth that reconnection in the boundary layer changes the wave spectrum and intensity and that the boundary layer is magnetically connected to the aurora. One would expect Saturn to have a boundary layer similar to that for Earth and Jupiter [see Tsurutani et al., 2001]. As discussed in Sittler et al. [2006], the rotational electric field is expected to dominate the convection electric field within Saturn's outer magnetosphere and prevent penetration of solar wind ions into Saturn's inner magnetosphere. Here we note that the Kelvin-Helmholtz instability at the dawn magnetopause [see, Goertz, 1983] may provide an important leakage of solar wind ions across the magnetopause into Saturn's magnetosphere. Magnetic field reconnection may be affected by occasional movement of the magnetopause across the orbit of Titan and its torus in response to variations in solar wind pressure. Solar wind ions can undergo charge exchange in the neutral torus and gain enhanced access as fast neutrals. This same process will produce ~ 50 keV N^+ pickup ions within the magnetosheath. Like the solar wind, these ions can re-enter the magnetosphere and contribute to the energetic particle population in the outer magnetosphere. Nitrogen ions picked up from Titan's nitrogen torus within the outer magnetosphere may diffuse radially inward while conserving the first and second adiabatic invariants. As this happens they will attain energies E ~ 100 keV at Dione's McIlwain L shell and E ~ 400 keV at Enceladus' L shell. The same will be true for O^+ ions picked up in the outer magnetosphere as previously discussed. With regard to N^+ pickup ions within the magnetosheath and their re-entry into the magnetosphere with conservation of their adiabatic invariants, they will acquire energies E ~ 1.6 MeV at Dione and E ~ 6.25 MeV at Enceladus. Other energization processes, such as substorms arising from inward convection of magnetotail plasma [Vasyliunas, 1970; Macllwain, 1974; Cowley et al., 2005] and acceleration by ELF/VLF waves [Summers et al. 1998], which are known to generate relativistic electrons within the Earth's magnetosphere are other possibilities.

The outline of the remainder of this paper is as follows: 1.) The Nitrogen Titan Torus, 2.) Voyager Ion Data at the Titan Torus, 3.) Voyager Ion Data at Dione's L Shell, 4.) Sources for Hot Plasma Ions within Saturn's Magnetosphere, 5.) Inward Transport and Loss of Suprathermal Ions, 6.) Ion Deposition Rates and Radiolysis as a Function of Depth for Dione's Surface, 7.) Present laboratory absorbance spectra based on energetic ion driven radiolysis with nitrogen as an important constituent in the ice, and 8.) Summary and Conclusions.

2.0 THE NITROGEN TITAN TORUS

Using the most recent estimates of the sputtering of Titan's atmosphere by UV photons and by the magnetospheric ions and electrons [Shematovich et al 2003] and the corresponding energy distribution of the ejecta, a Monte Carlo calculation of Titan's neutral torus was carried out. Although both N_2 and N are ejected, we assume in this model that nitrogen is fully dissociated for simplicity. The effect of the molecular nitrogen was described separately [Smith et al., 2004]. In Figure 1, a Monte Carlo calculation is shown of the atomic nitrogen torus and includes the gravitational fields of both Saturn and Titan as well as a neutral lifetime against ionization of $\tau_{N0} \sim 3 \times 10^8$ sec [Ip, 1992]. There is a concentration of atoms centered on Titan's L shell with peak densities ~ 20 atoms/cm^3, mean radial extent from 8 R_S and 25 R_S, vertical thickness of $\pm$ 2 R_S, and density concentrated at the equatorial plane, but some neutral trajectories extend all the way into Saturn's inner magnetosphere. The figure shows the neutral density as a function of radial distance and latitude. This will be used in the next section along with the observed suprathermal ion densities derived from the Voyager plasma data and corresponding radial diffusion resident time scales. This calculation is an improvement of that presented by Barbosa [1987] since it uses a realistic expression for the energy spectrum of ejected nitrogen atoms at Titan's exobase, displays their true radial and latitudinal dependence and includes a more realistic description of the gravitational field of the system. As expected, the solutions show a concentration of N atoms at Titan. The model calculations are run, until a steady state is achieved. The solutions are presented in 2D using a grid size of 320x300 cells with Titan fixed relative to Saturn in longitude, although the calculations were done in 3D with Titan orbiting around Saturn. Smith et al. [2004] also consider the variation of the ionization time scale as a function of radial distance and latitude. Here, the effects of the magnetopause boundary and bow shock also need to be considered for a truly 3D calculation. As noted above we estimate a torus, which is ½ the thickness of that estimated by Barbosa [1987] with a corresponding reduction of torus volume by factor of 4, giving an average neutral density of [N] ~ 10-20 atoms/cm^3.

Cravens et al. [1997] studied the possibility of other molecular species being ejected from Titan's exobase and contributing to the neutral torus and ion source. Future Monte Carlo calculations should include these species since their source strength may be as high as $S_M \sim 10^{25}$ molecules/s. These predictions will then be able to be compared with the ion formation rates to be measured by CAPS during the Cassini tour of the Saturn system.

3.0 VOYAGER ION DATA AT TITAN TORUS

In this section we will consider the Voyager observations of the plasma and energetic particle populations within the Titan torus region using the Voyager Plasma Science Experiment (PLS) observations [see Bridge et al. [1977]] and Low Energy Charged Particle Experiment (LECP) observations [see Krimigis et al., 1977]. These results will then be used with source rates presented in the previous section to estimate resident time scales of the ions within the torus region. We will also compare the two data sets together as a function of intensity versus energy and determine what assumed composition gives the best comparison of the two data sets across the energy gap separating the two data sets. PLS was able to discriminate between protons and heavy suprathermal ions because of Mach number effects, but for the LECP instrument this is more difficult. Maclennan et al. [1982] analysis of Voyager 1 LECP data for E > 30 keV centered on the Titan encounter period, estimated flow speeds ~ 200 km/s for the ambient plasma, consistent with that reported by Hartle et al. [1982]. They assumed protons and observed a slow down of the flow centered on Titan's orbit. We will also compare the temperatures of the suprathermal ions measured by PLS and the estimated pickup energies of the assumed ion species.

In Figure 2, we show a three-component Maxwellian fit to the Voyager 1 PLS data, for which the suprathermal component is assumed to be a heavy ion such as O^+ as shown by Cassini [Crary et al., 2005; Hartle et al., 2006]. These measurements were made near the equatorial plane in the Titan torus and would not provide a good fit for H^+ as the suprathermal component. The density for the suprathermal component is $[O^+] = 0.12$ ions/cm^3, with flow speed of 120 km/s and temperature $T_{O+} = 3.9$ keV. This temperature is close to the maximum pickup energy (i.e., v ~ 2V) for O^+/N^+ with a flow speed of 120 km/s. If we use the abundance of N^+ relative to O^+ as reported by Smith et al., [2005] of ~ 5% then $[N^+] \sim 0.006$ ions/cm^3. Hartle et al. [1982] reported that the plasma in the vicinity of Titan was hot and that flow speeds were between 80 km/sec and 150 km/sec with a mean speed of about 120 km/sec in agreement with Cassini results [Crary et al., 2005]. In this outer region we have a mixture of flux tubes with cold plasma and hot plasma and just hot plasma. The analysis by Richardson [1986] was primarily confined to plasma where cold plasma was present, densities higher and thus mass loading greater. So, we would argue that the results by Richardson [1986] had a selection effect for which it would tend to analyze those flux tubes with denser cold plasma, correspondingly greater mass loading and thus lower azimuthal speeds. Using our estimate of the ion density $[N^+]$, a neutral density $[N] \approx 40$ atoms/cm^3 from Figure 1, and ionization time τ_{N0} ~ 3 x 10^8 seconds, we estimate an N^+ ion residence time,

$$\tau_R \approx ([N^+]/[N])\tau_{N0} \approx 2.2 \times 10^4 \text{ seconds} \approx 7.4 \text{ hours}$$

We assume that this residence time is equivalent to the radial transport time via centrifugally driven transport, which dominates over other potential loss processes for the ions measured by PLS. The above estimate is comparable to the maximum radial diffusive transport time for O^+ ions from the OH neutral cloud model of Richardson et al. [1998], if we scale it relative to that at Dione's L shell where $\tau_R \sim 5$ days and assume an L^3 dependence for the radial diffusion coefficient. When we do this we get $\tau_R \sim 7.2$ hours

at L ~ 20. Here, we note that the source term for solar wind protons could be competitive with O^+/N^+ ions and yield similar resident time scales. As noted above, protons provide a poorer fit to the suprathermal ion component in the PLS spectrum shown in Figure 2. It is important to note that pickup ions initially form ring distributions [see Sittler et al. [2004a]] and are expected to pitch angle scatter into shell distributions [Vasyliunas and Siscoe, 1976a]. In Figure 3 we show a Voyager 2 PLS spectrum near Titan's L shell, but at high latitude. Here, we see no evidence of a suprathermal ion component. If steady state is assumed this indicates that the suprathermal O^+ ions are confined near the equatorial plane. This should also be true for suprathermal N^+, since our nitrogen torus calculations show the N atoms confined within 2 R_S of the equatorial plane. These observations also indicate that the pickup ions (O^+/N^+) retain their initially large perpendicular energy relative to the planetary magnetic field (i.e., $T_\perp / T_{ll} >> 1$) and that formation of shell distributions from ion scattering is not dominant (i.e., if scattering was effective, both the O^+ and N^+ would be made isotropic since they are of similar mass). Sittler et al. [2004a, 2005b] showed that finite gyro-radius effects were important and that the hot keV ambient ion component had to be a heavy ion such as N^+/O^+ with ion gyro-radius r_g ~ 5600 km. This has since been confirmed by Hartle et al. [2006].

Compared to the radial diffusion coefficient $D_{LL} \sim 5x10^{-7}$ R_S^2/s used for Richardson et al.'s OH model, Paranicas and Cheng [1997] used ~ 10^{-7} R_S^2/s to fit measured phase space density profiles for ~ 100-keV O^+ from Voyager LECP measurements in the macrosignature region of Enceladus. However, there is great uncertainty in using moon absorption signatures of energetic particles [e.g., Paranicas et al., 1997] to determine transport rates without quantitative estimates for injection rates at these energies from distributed sources such as E-ring grain sputtering [Jurac et al., 2001a,b]. Apparent radial dependence of radial diffusion rates for loss-less diffusion can arise from radial variation of source and loss rates. This was strongly suggested by the phase space density analysis for LECP ion and electron data of Armstrong et al. [1983], who derived diffusion rates increasing towards Saturn for loss-less diffusion and highly contrary to known diffusion models, all with positive radial gradients in D_{LL}. Diffusion rates may also be strongly dependent on energy and momentum. Cooper [1983] and Randall [1994] respectively derived diffusion rates for high energy protons and electrons, both explicitly using models for sources of these particles from cosmic ray albedo neutron decay (CRAND) in the inner magnetosphere, in the range $D_{LL} \sim 1 - 3 \times 10^{-10}$ R_S^2/s near Enceladus, three orders of magnitude less than the results from Voyager PLS and LECP. Finally, apparently high diffusion rates can be derived from moon microsignatures [e.g., Carbary et al., 1983; Paranicas and Cheng, 1997] on the assumption that electron and ion drift shells have longitudinal symmetry, but Cooper et al. [1998] has demonstrated that this assumption can be dramatically violated for keV-MeV electrons due to effects of global electric fields in the magnetosphere. In the most extreme cases, for electron energies near longitudinal drift resonance where corotational motion is cancelled by equal and opposite gradient curvature drift, the electron drift shells close in banana-shaped configurations on the dusk side of Saturn and do not extend fully around to the dawn side. Dawn-dusk asymmetries in intensities and phase space densities of keV-MeV ions [Krimigis et al., 1983] and electrons [Maurice et al., 1996] generally suggest that longitudinal symmetry of global transport is a poor assumption. These issues will have important implications

when we discuss various source and loss mechanisms for the charged particle populations in sections 4 and 5.

In Figure 4 we show a combined plot of the PLS and LECP ion data in the Titan torus region where N^+/O^+ ions are assumed both for the PLS suprathermal component and for the LECP data. We used the calibration data for heavy ions presented in Krimigis et al. [1981] paper for Jupiter's magnetosphere for our analysis of the LECP data. For these calculations we used raw count rate data, which is independent of composition and removed data from one directional sector, sector one, which is contaminated from sunlight entering the sensor. Background corrections from energetic electrons in this region are estimated to be negligible, for both instruments but are important in the inner magnetosphere [Paranicas et al., 1997]. We used 30-minute averages. We have also super-imposed the PLS-LECP electron intensities from Maurice et al. [1996] for both Voyager 1 and 2. The PLS ion data has been converted from instrument currents to particle intensities.

When one compares the energy spectrum across the energy gap between the two instruments, the comparison is very good. If we assume that protons dominate the suprathermal ions the comparison is not as good. The comparison between PLS and LECP across the energy gap is evidently not satisfactory. Furthermore, if one uses the 500 keV proton intensities measured by the LECP channel 32 as reported by Krimigis et al. [1983], they are only 10% of those estimated here for N^+/O^+. However, protons may very well dominate the spectrum at high energies if the source of these ions is the solar wind and there is efficient access into Saturn's outer magnetosphere. Here we refer one to the classical papers by McIlwain [1974] and Vasyliunas [1970, 1975, 1976b]. Magnetospheric convection can be an important process for accelerating solar wind protons and alphas within Saturn's magnetosphere similar to that for the Earth's magnetosphere. But, as discussed in the next section the defining parameter is the ratio of the convection electric field relative to the rotational electric field within Saturn's outer magnetosphere. As previously noted, the analysis by Maclennon et al. [1982] favored a composition dominated by protons for $E > 30$ keV within the Titan torus. Therefore, the composition of these energetic ions in the outer magnetosphere cannot be determined with certainty at this time. Initial energetic particle results reported by Krimigis et al. [2005], indicates comparable amounts of protons and water group ions.

If the high energy component observed by LECP is dominated with N^+/O^+ ions, then these high energies could be the result of turbulence in the outer magnetosphere acting on pickup N^+/O^+ ions as the seed population. For example, the N^+/O^+ ions could satisfy a bounce resonant interaction with ULF waves in the outer magnetosphere [see Schultz and Lanzerotti, 1973]. The Voyager magnetometer data does show the presence of turbulence in the outer magnetosphere [Lepping et al., 2005], which could indicate VLF or ULF waves or compression-expansion episodes of the magnetosphere caused by the solar wind interaction [Southward and Hughes, 1983; Hughes, 1994; Anderson, 1994; Sibeck, 1994; Mathie and Mann, 2000]. More comprehensive magnetometer data for wave analysis is now becoming available from the Cassini orbiter which is now in orbit around Saturn (i.e., orbit insertion with Saturn occurred on July 1, 2004). As discussed in section 1.2

and in section 4.2 and 4.3, N^+ ions born within the magnetosheath can have pickup energies ~ 50 keV and then enter the magnetosphere similar to that for solar wind ions where they can be further energized. It is also important to note that the ion pressure in the LECP data near Titan's orbit is about 50% of that below 10 keV, although a majority of the ion density is below 10 keV. The total ion pressure is ~ 0.2 nPa, the total electron pressure is ~ 0.01 nPa and the magnetic field pressure is ~ 0.01 nPa. Therefore, the plasma beta is estimated to be $\beta >> 1$. This equipartition of energy between the low energy plasma and hot plasma is similar to that observed for the electron component of Saturn's magnetosphere as reported by Maurice et al. [1996].

4.0 SOURCES FOR HOT PLASMA IONS WITHIN SATURN'S MAGNETOSPHERE

Here, we discuss the various sources of suprathermal ions within Saturn's magnetosphere, and how they may be accelerated to very high energies. In the case of solar wind protons it provides a framework for how to estimate the entry of pickup N^+ ions born within Saturn's magnetosheath and how sub-storms can further energize the suprathermal populations. Radial transport (i.e., flux tube inter-change motions and charge-exchange transport to name a few) plays a very important role with regard to further energization of the ions and formation of Saturn's radiation belts. This will then lead into the possible implantation of energetic nitrogen ions within the icy surfaces of Saturn's moons, which can then be sputtered and form low energy nitrogen ions within Saturn's inner magnetosphere as observed [Smith et al., 2005]. This can complicate the identification of primordial ammonia that may be trapped within the interiors and surfaces of Saturn's moons.

4.1 Solar Wind Source

A solar wind source (i.e., protons and alphas) within Saturn's outer magnetosphere can provide keV and hotter protons. The source strength for solar wind protons can be roughly estimated using the following expression

$$S_{SW} \approx (N_{SW}V_{SW})(\pi(R_M/2)^2)(1/2)\varepsilon$$

The ½ factor is used since half the time the solar wind B_Z will point northward for reconnection on the front side magnetosphere and solar wind entry into the magnetosphere and southward for a closed magnetosphere with no entry into the magnetosphere. At Saturn N_{SW} = 0.05 ions/cm^3, V_{SW} = 400 km/s, R_M = 20 R_S and ε = efficiency for solar wind entry into Saturn's magnetosphere. At Earth $\varepsilon \approx 0.05$ and the efficiency goes like $1/M_A$ (M_A = Alfven Mach number in the solar wind = $V_{SW}/V_A \approx 10$) [see Slavin and Holzer, 1979] which reduces ε by 1.5 relative to that at Earth, so $\varepsilon \approx 3$ %. For this value of ε we get $S_{SW} \approx 4x10^{26}$ ions/sec. In addition, $E_{cor} >> E_{conv}$ at Saturn, so this efficiency could be lowered by an additional factor β, where $0.01 < \beta < 1.0$. This parameter, applicable near the magnetopause boundary, is essentially unknown and probably will require composition measurements by CAPS during the Cassini tour of Saturn's magnetosphere. If we assume $\beta \sim 0.1$, then we get $S_{SW} \sim 4x10^{25}$ ions/sec.

4.2 Titan Torus Source

The source strength for the nitrogen torus is $S_{N+} \approx (4.25 \times 10^{25}$ ions/sec)(2/3) = 2.8×10^{25} ions/sec [Note, the factor of 2/3 is used since part of the neutral torus can extend into the magnetosheath]. Therefore, the source strength of the suprathermal keV N^+ ions is about the same as that for solar wind keV protons. Titan's hydrogen torus is not considered since pickup energies are about 100 eV and therefore do not correspond to the suprathermal ions observed by PLS within the Titan torus region. In the case when the magnetopause is pushed inside of Titan's L shell, charge exchange reactions will produce within the magnetosheath ~ 50-100 keV N^+, ~ 4 keV H^+ pickup ions (i.e., $V_{SH} \sim 400$ km/s) and energetic atomic hydrogen atoms, $E_{H*} \sim 1$ keV that would be ejected from the Saturn system. The pickup N^+ ions would tend to be convected away by the magnetosheath flow, but some could enter the magnetosphere, similar to solar wind protons, with very high injection energies $E_{N*} \sim$ 50-100 keV and higher since the polar cap potential could exceed 400 kV (see later discussions). The importance of this source of energetic N^+ ions and H^+ is difficult to estimate, but could be as high as $S_{N*+} \sim 3 \times 10^{23}$ ions/sec for N^+ and $S_{H+} \sim 4 \times 10^{24}$ ions/s for H^+ (i.e., density of hydrogen cloud $N_H \sim 20$ atoms/cm^3). The N^+ ions could contribute to the energetic ions observed by LECP, while the H^+ ions could contribute to the suprathermals observed by PLS within Saturn's outer magnetosphere. This relatively large injection of energetic particles would only occur during the passage of compression regions and coronal mass ejections (CMEs). Although, temporal, they could contribute to the more permanent energetic populations within Saturn's magnetosphere. Since, part of the torus is always in the magnetosheath plasma regime, a smaller energetic source of N^+ ions will always be entering Saturn's outer magnetosphere and contribute to its energetic population. If the neutral clouds of atomic oxygen also extend into the magnetosheath then the pickup O^+ from these clouds will experience a similar energization as the N^+ and enter the magnetosphere similar to that for solar wind protons and alphas with a source rate during storms $S_{O*+} \sim 6 \times 10^{24}$ ions/s.

4.3 Sub-Storms and Charged Particle Energization

It is important to consider the possibility of sub-storms at Saturn and the consequences they will have on the charged particle populations and their energetics within Saturn's magnetosphere. During the growth phase of substorms at Saturn we expect to have time scales $\tau_G \sim (2\pi B_T R_M)/(B_{SW} V_{SW}) \approx 2$ days ($B_T = 3$ nT, $B_{SW} = 0.5$ nT, $R_M = 20\ R_S$, $V_{SW} =$ 400 km/s). In the case of the Earth, $\tau_G \sim 2.5$ hours, while for Mercury we expect $\tau_G \sim$ 1-2 minutes [Siscoe et al., 1975]. We estimate the time scale for an injection event after sub-storm onset to be $\tau_I \geq 2$ hours when neglecting line tying effects (i.e., this time scale could be longer), while for Earth the injection time scales $\tau_I \sim 40$ minutes or less [McPherron, 1997; McPherron et al., 1986]. As estimated above, the polar cap potential drop $\Delta\Phi_{PC} \approx (V_{SW} B_{SW})(2R_M)\eta \approx 48$ kV for which we set $\eta \approx 0.1$ [Tsurutani and Lakhina, 1997]. This large potential drop across the polar cap can energize solar wind ions to very large energies via the return flow from the magnetotail [see Vasyliunas, 1970; Vasyliunas, 1975; Vasyliunas, 1976]. Using the poynting flux as described by Siscoe et

al. [1975], the total input power is $W \sim R_M \Delta\Phi_{PC} B_T/\mu_0 \approx 1.4x10^{11}$ watts, very close to the EUV aurora power reported by Broadfoot and Sandel [1981] of ~ $2x10^{11}$ watts. If we use a solar wind source at the magnetopause or boundary layer of $S_{SW} \sim 4x10^{26}$ ions/s and use a power input due to convection of $W \sim 1.4x10^{11}$ watts, we get a mean energy of solar wind protons of $E_P \sim 2.5$ keV. This estimate is comparable to their mean energy of $E_P \sim 1$ keV in the solar wind. If, we use the lower estimate for the solar wind source, then the protons will be energized to $E_P \sim 25$ keV, which is comparable to the polar cap potential. At the orbit of Titan the rotational electric field $E_{rot} \approx V_{rot} B_{Titan} \sim 300\text{-}600$ μV/meter (V_{rot} ~ 60-120 km/s, $B_{Titan} \approx 5$ nT), while the convection electric field $E_{conv} \approx (V_{SW} B_{SW})\eta \sim 20$ μV/meter << E_{cor} as previously argued. The parameter η is highly uncertain. During the passage of a compression region and if we assume a jump in B and density by a factor of 4, [Smith et al., 1980], then the convection electric field could increase to $E_{conv} \sim 160$ μV/meter and start to be competitive with the rotational electric field (as discussed in Sittler et al. [2006], this is offset by the spinning up of the magnetosphere as it is compressed). Futhermore, the merging rate efficiency at the magnetopause is inversely proportional to the Alfven Mach number [Slavin and Holzer, 1979], which could decrease by a factor of two within a compression region, and increase $\eta \sim 0.1$. Therefore, the number of particles entering the magnetosphere could increase by a factor of 16 (i.e., β factor also increased by factor of 2), the polar cap potential to $\Delta\Phi_{PC} \sim 400$ kV (i.e., charged particle energization) and the input power to $W \sim 1.1x10^{12}$ watts and resulting in auroral brightening. This argument is similar to that proposed by Cowley et al. [2005] to explain the auroral events observed during the HST-Cassini campaign in January 2004. Sittler et al. [2006] have argued that most of the auroral brightening can be traced to a centrifugal instability mechanism and Kelvin-Helmholtz instability at dawn magnetopause as originally discussed by Goertz [1982] and Curtis et al. [1986]. The effectiveness of the return flow can be traced to the parameter $\beta \sim E_{conv}/E_{cor}$. If there is no return flow, then the hot N^+ ions would be ejected down the tail as part a magnetospheric wind similar to that observed by Sittler et al. [1987] for the Jovian tail.

The presence of boundary layers at all planetary magnetospheres are expected to be present, for which the low latitude boundary layer (LLBL) plays a most critical role with regard to magnetospheric convection and substorm phenomena [Tsurutani et al., 2001; Sonnerup and Siebert, 2003]. The LLBL can also be an important source for ELF/VLF plasma waves within the outer magnetosphere and result in crossfield diffusion (i.e., turbulent electric fields) of ions and electrons into the magnetosphere (i.e., boundary layer thickness) where they can be further energized via field aligned electric fields and corresponding auroral brightenings [Tsurutani et al., 2003]. Once these particles have entered the magnetosphere, they can be further energized by magnetospheric convection processes. One of the primary objectives of the Cassini mission is to provide a more accurate estimate of the parameter η, related to the ε parameter noted above, and to search for the presence of a boundary layer during magnetopause crossings.

5.0 Inward Transport and Loss of Suprathermal Ions

Up till now we have focused our discussions with regard to the sources of suprathermal ions within Saturn's outer magnetosphere and their energization. Here, we briefly comment on the inward transport of the suprathermal ions and their entry into the inner magnetosphere where they can contribute to Saturn's inner radiation belts. During inward radial transport they must deal with various losses such as satellite sweeping, collisions with dust and neutral clouds and precipitation into Saturn's atmosphere via wave-particle interactions. These calculations are part of a separate publication [Sittler et al., manuscript in preparation, 2006] where an in-depth study of the above processes are performed and their relative importance between protons and heavy ions such as O^+/N^+ are considered.

In summary, we find that satellite sweeping calculations for Rhea are not important for N^+ with transport time scales $\tau_R \sim 10$ days. Lepping et al. [2005] did an in-depth study of MHD waves from $8.5 < L < 16.9$. These waves can pitch angle scatter the N^+ ions and precipitate them into Saturn's atmosphere. MHD waves are observed to be important near the outer boundary of the plasma sheet at $L \sim 15$. Using the Richardson et al. [1998] results, we estimated a lower limit for the predicted radial transport time scale $\tau_R \sim 2$ days at $L \sim 8.5$. If so, then both precipitation and satellite sweeping by Rhea of the suprathermal ion population would be negligible at $L \sim 8.5$. However, this is contrary to observations [see, Armstrong et al. [1983] and Paonessa and Cheng [1986a,b]]. Richardson et al. [1998] did indicate that their model predictions would be more consistent with observations if radial transport declines with increasing distance between 7 and 12 R_S. One possibility for this they said was that the transport rate was dependent on the mass-loading rate. This is consistent with the OH and water group neutral clouds being confined within $L \sim 7$ [Richardson et al., 1998] and the Titan neutral tori being confined outside $L \sim 12$ [Barbosa, 1987; Ip, 1992 and this work]. This result is also consistent with the analysis by Lepping et al. [2005] where wave activity does not seem to be important between L ~ 7-12. Furthermore, radial diffusion rates may decrease with increasing charged particle energy (i.e., E ~ 50 keV versus E < 10 keV). Therefore, the data when combining all observational constraints is consistent with radial transport time scales $\tau_R \sim 10$ days at $L \sim 8.5$. Otherwise, the transport rate from Richardson et al. [1998] would be applicable. Finally, we note that the neutral hydrogen cloud, which has been reported from Voyager UVS data [Shemansky and Hall, 1992] to extend throughout Saturn's magnetosphere, is not expected to be an important source of mass loading and the suprathermal populations discussed here, due to low mass. But, it could be an important charge exchange sink for suprathermal and energetic protons and heavy ions.

6.0 VOYAGER ION DATA AT DIONE'S L SHELL

In this section we examine the ion measurements in the vicinity of Dione's L shell, in the context of our proposed model where suprathermal N^+ ions originate within Titan's neutral torus and then diffuse radially inward to contribute to Saturn's inner radiation belts. We will also explore various loss mechanisms for these nitrogen ions and the "solar wind" protons. This will provide further constraints on the radial diffusion coefficients.

In Figure 5 we show a three-component Maxwellian fit to the PLS ion data at the Voyager 1 outbound Dione L shell ring plane crossing. The PLS instrument includes four Faraday cup sensors (A-D) aligned in different directions. Within Saturn's magnetosphere the D cup is directed upstream towards the incoming rotating flow and is usually exposed to the highest ion fluxes, while A, B and C are pointing nearly perpendicular to this direction. Here, the suprathermal ion is assumed to be H^+, but the fit for this component, particularly in the D cup, is poor. In Figure 6 we show a fit to the same data, but now assuming N^+ for the suprathermal ion component. The fit is significantly better than that for H^+, especially in the D cup spectrum. In theory, we would expect a better fit assuming a water group ion for the suprathermal component, since within Saturn's inner magnetosphere one expects the neutral clouds to be dominated by water group molecules and atoms such as O^+, OH^+, H_2O^+ and H_3O^+ [see Young et al., 2005; Sittler et al., 2005a]. The density of the suprathermal component is $[O^+] \approx 3.9$ ions/cm^3, while the temperature of the O^+ suprathermal component is $T_{O+} \approx 2$ keV. The maximum pickup energy for H_2O^+ ions at Dione's L shell is $E_{MAX} \approx 1.4$ keV for a ring distribution, which is consistent with the observed temperature.

In Figure 7, we show a combined plot of PLS and LECP data during Voyager 1's outbound crossing of Dione's L shell, also near the ring plane crossing of this spacecraft. Water group ions are assumed for the PLS suprathermal ion component and LECP data above 10 keV was assumed to be dominated by O^+/N^+ [Krimigis et al., 2005]. The comparison across the energy gap looks good with a common power law between 1 keV and 3 MeV. Conserving the 1st and 2nd adiabatic invariants, using the mean energy of the PLS suprathermal O^+/N^+ component at Titan's torus and mapping to Dione's L shell, we obtain a mean O^+/N^+ energy greater than 100 keV. This would suggest that most of the LECP fluxes are O^+/N^+. However, Paranicus et al. [2004] suggested that for energies greater than 500 keV, the composition is dominated by protons. Cassini results have not yet been presented to confirm or deny their conclusion that protons dominate at E > 500 keV. We have also super-imposed the electron intensities from Maurice et al. [1996]. These electrons will be important for the radiolytic reactions taking place for depths greater than 1 micron in the surface ice of Dione.

Pressure integrals over the Dione PLS spectra depend strongly on whether the ion is H^+ or O^+, the latter giving 2.6 nPa as compared to 0.1 nPa for H^+ at plasma energies and 1.1 nPa for the LECP ions inferred to be O^+/N^+. For O^+ this result differs from integrals for the Titan O^+/N^+ spectra giving comparable 0.1 nPa pressures at both PLS and LECP energies. In contrast, Maurice et al. (1996) found comparable pressures for plasma and energetic components of the electron population in Saturn's middle magnetosphere. The electron pressure is ~ 0.2 nPa. For magnetic pressure $B^2/8\pi \sim 2.5$ nPa at Dione's orbit the plasma β parameter, the ratio of plasma and magnetic pressure, is ~ 1 for an O^+ plasma component, 0.44 for energetic O^+/N^+, 0.08 for electrons and ~ 1.5 overall. Due to low magnetic field at Titan's orbit the $\beta \sim 10$ values are much higher, but even at Dione high β effects such as diamagnetism may be present.

In Table 2 we summarize the particle and field parameters that characterize the environment surrounding Dione.. The ion and neutral densities were derived from

Richardson et al., [1998] and this paper. More recent results from Jurac and Richardson [2005] are indicated in parenthesis for the ambient ions and neutrals. However, for our purposes either could apply. In Jurac and Richardson [2005] they have increased the source of water to the magnetosphere from $S_W \sim 10^{27}$ mol/s from Richardson et al. [1998] to $S_W \sim 10^{28}$ mol/s, with very high neutral densities near Enceladus ~ 5900 mol/cm^3.

Table 2

Parameter	Value
L	6.3
N_e (#/cm^3)	35.0
T_e (eV)	10.0
[H^+] (#/cm^3)	2.1
[O^+] (#/cm^3)	23.0 (4.0)
[OH^+] (#/cm^3)	3.5 (13.0)
[H_2O^+] (#/cm^3)	2.8 (12.0)
T_{H+} (eV)	51
T_{O+} (eV)	261
T_{OH+} (eV)	278
T_{H2O+} (eV)	294
[O^+]* (#/cm^3)	3.9
T_{O+}* (eV)	2000.0
[H] (#/cm^3)	80.0 (15.0)
[O] (#/cm^3)	180.0 (45.0)
[OH] (#/cm^3)	250.0 (150.0)
[H_2O] (#/cm^3)	30.0 (75.0)
V_R (km/s)	53.0
B (nT)	80.0

* indicates suprathermal component

7.0 ION DEPOSITION RATES AND RADIOLYSIS AS A FUNCTION OF DEPTH FOR DIONE'S SURFACE

In this section we will estimate the ion implantation rates and radiolysis as a function of depth for the icy surface of Dione using the intensities shown in Figure 7 and the published electron intensities by Maurice et al. [1996] which covers the energy range from 10 eV to 2 MeV. Below 10 keV we used the composition shown in Figure 6 for PLS where the suprathermal component is assumed to be N^+/O^+, while at energies greater than 10 keV we assumed a similar composition of N^+/O^+. Delitsky and Lane [2002] assumed the nitrogen was 10% of the thermal plasma. Cassini plasma measurements [Smith et al., 2005] and energetic particle measurements [Krimigis et al., 2005] indicate that N^+ is ~ 5% of O^+ at all energies. As reported in Richardson et al. [1998], the source of water molecules within Saturn's inner magnetosphere is $S_W \sim 1.4 \times 10^{27}$ mol/s (Jurac

and Richardson, 2005 have increased this estimate to $S_W \sim 10^{28}$ mol/s), while the source of hot nitrogen atoms within Saturn's outer magnetosphere is $S_{N*} \sim 4.5x10^{25}$ atoms/s. Potential sources of hot O neutrals with $S_O \sim 6x10^{26}$ mol/s are expected to populate the outer magnetosphere via charge exchange transport [see Johnson et al., 2005]. The hot N^+/O^+ ions from the neutral torus will be transported outward and lost to the magnetopause. But, the recent Cassini results by Burch et al. [2005] show that hot plasma can be injected into the inner magnetosphere, where they can be energized as previously discussed. The calculations by Smith et al. [2004] show significant production rates of nitrogen pickup ions as close in as Dione, indicating that there could be an important source of low energy nitrogen ions from Titan in Saturn's inner magnetosphere. For our ion implantation and radiolysis calculations we will use the codes developed by Cooper et al. [2001] for the icy Galilean satellites.

In Figure 8 we show the ion implantation rate in terms of ion density per year as a function of surface depth. It is useful to know for the following discussions that the column density of water molecules in ice for a depth of 1 cm is $\sim 3 \times 10^{22}$ mol/cm^2. We will use 10% of this as an upper estimate for our accumulated implanted column densities for N^+ within the ice and corresponding accumulation time scale τ_{acc}. Figure 8 shows that within a few mono-layers of the surface the plasma ions O^+ and H^+ dominate the implantation of ions and the corresponding accumulation time scales $\tau_{acc} \sim 1.2$ Myrs for O^+ , $\tau_{acc} \sim 24$ Myrs for N^+ and $\tau_{acc} \sim 3$ Myrs for H^+. The energetic O^+/N^+ will penetrate below 1 micron, with an effective accumulation time $\tau_{acc} \sim 30$ Myrs for O^+ and 600 Myrs for N^+. The time scale for meteoritic gardening over a depth of 1 cm is about 10^4 years [Cooper et al., 2001], which is far shorter than our implantation time scales. Therefore, it is reasonable to assume that the implanted oxygen and nitrogen will be uniformly distributed over such a depth. For longer time scales the meteoritic gardening will extend down to ~ 1 meter depth. Cooper et al. [2001] also argue that these ions will be buried faster by impact ejecta than they can removed by sputtering or sublimation. Actual regolith depth depends on geologic age of the surface, which in the case for Dione is > 1 Byrs [Morrison et al., 1984]. This argument should be even more applicable at Saturn where the icy satellites are colder and the sputtering rates are considerably less than that at the Galilean satellites, except for may be Callisto. The gravitational focusing factor, used for the above calculations, $f_G \sim 1 + (v_{esc}/v_\infty)^2 < 1.7$ at Saturn. This estimate is comparable to but less than that for Jupiter with $f_G < 2.8$ for Europa, Ganymede and Callisto [Cooper et al., 2001]. At Saturn we use $v_{esc} \sim 12$ km/s (i.e., at Rhea's orbital position) and $v_\infty \sim 14$ km/s. Therefore, meteoritic impact rates at Saturn are comparable to but less than that at Jupiter, but more than offset by the higher sputtering and sublimation rates for the Galilean icy satellites.

Delitsky and Lane [2002] suggest a chemistry model that might occur due to nitrogen implanted into the water ice. The nitrogen was first converted into nitric oxide, NO, and then into other nitrogen molecules. Here we note that since the O^+ fluences are so much larger than that for N^+, molecules such as hydrogen peroxide, H_2O_2, may dominate the nitrogen compounds in the ice. Molecular oxygen, a by-product of hydrogen peroxide has been detected at Ganymede [Spencer et al., 1995] and ozone, produced by photolysis of O_2, has been detected at Rhea and Dione [Noll et al., 1997]. In Figure 9, similar to that

done for Figure 8, we show the dosage time for radiological processes to occur for Dione, using the ion and electron intensities shown in Figure 7. For depths greater than 1 mm, the radiolysis is dominated by the energy deposited by penetrating energetic electrons [see Johnson et al., 2004]. At depths, ~ 1 micron, the energetic oxygen ions dominate the radiolysis, while within a few mono-layers of the surface plasma oxygen and protons dominate the radiolysis. Near the surface the dosage time scale at 0.1 microns is about 50 years, while at Europa it is about 3.5 years and Callisto about 150 years. At 1 micron the radiolysis time scale, is about t ~ 500 years. By using the intensities shown in Figure 7, the nature and depth distribution of the energy deposition is different from that used by Delitsky and Lane [2002]. But, most importantly, our estimated net energy fluxes are greater by an order of magnitude than those in Delitsky and Lane [2002]. In the case of ion energy flux they estimated an energy flux ~ 1.7×10^8 keV/cm^2-s, while we estimate an energy flux ~ 6.5×10^7 keV/cm^2-s for the thermal plasma and ~ 5.5×10^7 keV/cm^2-s for the E > 10 keV hot plasma, for total ion energy flux ~ 1.3×10^8 keV/cm^2-s. In the case of electrons we estimate an energy flux for PLS electrons ~ 2.6×10^8 keV/cm^2-s and for the LECP-CRS electrons we estimate ~ 1.5×10^9 keV/cm^2-s, for a total electron energy flux ~ 1.8×10^9 keV/cm^2-s. In the case of Delitsky and Lane [2002], they estimated an electron energy flux ~ 2.2×10^8 keV/cm^2-s, which is an order of magnitude lower than our estimate. To compute our energy flux, EF, we used the expression

$$EF = \pi \int j(E) E dE$$

for which E is the particles relativistically correct total kinetic energy [see Cooper et al., 2001]. This integral has a stronger weighting at higher energies than that used by Delitsky and Lane [2002]. As expected, their numbers are closer to what we call the contribution from PLS, where most of the electron density resides. The electron energy spectrum is highly non-Maxwellian, and accounts for the large discrepancy.

For an individual species, Delisky and Lane [2002] estimated the column densities for a wide range of molecules using the formula N = EGt, for which, E is the energy flux (keV/cm^2-s), G is the radiolysis yield or "G value" in units of molecules/100 eV of energy deposited, and t is the time. This is applicable only if the percentages are very small. They used t =1000 years, which is subjective, but comparable to the meteoritic gardening time scale at a depth of 1 mm [see Cooper et al., 2001], which is essentially the optical depth for composition measurements if grain sizes for optical scattering are something like 100 microns. Because our energy flux is an order of magnitude greater than theirs, we need use a time t ~ 100 years in order to get molecular abundances similar to that computed by Delitsky and Lane [2002]. We have converted their numbers to a percentage of the column density for ice $N_W \sim 3.3 \times 10^{22}$ mol/cm^2. This was done as a means of estimating what fraction of the water molecules sputtered into Dione's atmosphere is composed of these molecules, and whether the Cassini Plasma Spectrometer (CAPS) Ion Mass Spectrometer (IMS) will be able to detect them as pickup ions [see Sittler et al., 2004a]. If we sum up all the molecules relative to the water molecules in the ice we get 21.7% of all the water molecules being composed of the various molecules listed in Delitsky and Lane [2002]. This large percentage violates the original assumption made when using these G factors and underscores the fact that one

cannot decouple the reaction between the various species derived by Delitsky and Lane [2002].

Sputtering is an important loss mechanism for the icy surface of Dione removing implanted ions and producing resultant chemistry in the ice. For example, the sputtering rate is $F_D \sim 5x10^8$ mol/cm^2/s (Jurac et al., 2001a,b), so that the time scale to remove 1 cm of ice from Dione's surface is $\tau_{sput} = N_W/F_D \sim 10^6$ years << $\tau_{acc}(N^+) \sim 600$ Myrs). But, the rate of meteoritic gardening down to a 1 cm depth is $\sim 10^4$ years, which is << τ_{sput}. So, the various nitrogen and hydrocarbon molecules could be buried deeper in the ice and survive losses due to sputtering. We should also note that the sputtering rates are higher for those molecules that are more volatile or outgas at higher rates for formation of an exosphere or corona around Dione [see Sittler et al., 2004b]. To estimate the neutral density of this corona, we assume a source rate ~ 10^{26} mol/s, which are only due to sputtering of ice, are added to the gas phase at Dione. We then need to estimate scavenging time scale for removing the atmospheric molecules. This is related to the charge exchange lifetime $\tau_{cx} \sim 2x10^6$ s [Richardson et al., 1998], ionization time scale $\tau_{ion} \sim 5 \times 10^6$ s [Richardson et al., 1998] and the elastic scattering time scale $\tau_{elastic} \sim 1.8x10^6$ s (i.e., used collision cross-section $\sigma \sim 3x10^{-15}$ cm^2 from Eviatar and Podolak (1983) and Book (1977)), which gives us an overall scavenging time scale of $\tau_{scav} \sim 8x10^5$ s. The estimated scale height of this atmosphere is h ~ 120 km. Combining these we can estimate the atmospheric density $n = (10^{26})(8 \times 10^5)/(5.8x10^{23}$ cm$^3) \sim 10^8$ mol/cm^3. Evidently, if true, this atmosphere was not detected by Voyager. This estimate is lower by several orders of magnitude than that given by Sittler et al. [2004b], who based their estimate, $n \sim 8x10^{11}$ mol/cm^3, on an observed column density of $\sim 2 \times 10^{16}$ mol/cm^2 for ozone in ice at Dione which roughly corresponds to a column density of O_2 trapped in ice $\sim 10^{19}$ mol/cm^2 [Noll et al., 1997]. This gives an upper estimate with the actual atmospheric density probably resides between these two limits and its detection by Cassini should be a high priority. In order for CAPS to detect nitrogen based molecules their number should be at the 1% level or greater relative to the number of water molecules in the ice. Also, CAPS should be able to detect an atmosphere or corona as estimated here and in Sittler et al. [2004b]. Our calculations do indicate that species such as N, NO, NO_2, HNO_3, N_2, and N_2O if at the 1-10% level relative to water ice, should be detectable by CAPS.

Delitsky and Lane [2002] did not assume the presence of ammonia in the ice from the primordial formation of the Saturn System. The presence of ammonia within Titan's crust is thought to be significant because of its dense N_2 atmosphere [e.g., Sittler et al., 2004b] and it has been proposed that the activity observed by Encleadus' could be due to ammonia [e.g., Stevenson 1982]. We also note, that the dominant ion within Titan's ionosphere may not be N_2^+, but rather H_2CN^+ [Hartle et al., 1982; Keller et al., 1998], $C_2H_5^+$ [Keller et al. 1992] and CH_5^+ (the latter can dominate at higher altitudes) [Keller et al., 1998]. Furthermore, methane ions have been observed within Saturn's outer magnetosphere and pickup region around Titan as observed by Cassini [Crary et al., 2005; Hartle et al., 2006] and predicted by Sittler et al. [2005b] based on Voyager 1 encounter data with Titan. Therefore, like the N^+ discussed here significant amounts of C^+ could be present in the inner magnetosphere. Delitsky and Lane [2002] assumed that

CO_2 was already present in the ice. Up till now the C^+ has not been detected by Cassini within the inner magnetosphere.

8.0 LABORATORY EXPERIMENTS PERFORMING ION IRRADIATION-RADIOLYSIS OF ICY SURFACES AND MEASURING IR ABSORBANCE SPECTRA FOR SURFACE COMPOSITION MEASUREMENTS.

Saturn's icy satellites, when implanted with nitrogen are expected to produce new molecules in an ice matrix or as inclusions in ice. We now consider some laboratory data using irradiation techniques developed by Moore and Hudson [2000] to confirm the possible presence of the nitrogen species discussed above. At present, only MeV protons are used in laboratory ice irradiations and IR spectroscopy is used to follow the corresponding chemistry that results. In terms of estimating the effect of radiolysis and corresponding chemistry for the same dose the energetic protons produce to first order the same effect as the energetic oxygen and nitrogen ions. The implantation of N^+ and O^+ in the ice can be simulated by mixing N_2 and O_2 in the ice and then irradiating this ice mixture with energetic protons. To determine likely products, we examined an ice mixture of $H_2O + N_2 + O_2$ (3:1:1). When such a laboratory ice is condensed at 20 K and warmed to 100 K (a temperature more relevant to the icy surfaces at Saturn), most of the N_2 and O_2 sublime. If irradiations are performed at 100 K there is not enough N_2 and O_2 trapped in the ice to make IR-detectable products. Therefore, we irradiated the ice mixture at 20 K. Figure 13 shows the products observed, NO, NO_2, N_2O, O_3 and H_2O_2, which have lower vapor pressures than N_2 and O_2. When the irradiated sample was warmed to 100 K, N_2O, O_3 and H_2O_2 were still observed. Therefore, several of the species discussed by Delitsky and Lane [2002] were observed in this simulation. Most of the G factors used by Delisky and Lane [2002] were inferred from related experimental data, so there is considerable uncertainty. The results shown in Figure 10, shows some of the molecules produced in the ice, such as NO and NO_2, could sublimate from the ice and contribute to an exosphere or corona around Dione (see previous section). Meteoritic gardening will tend to mix these molecules to depths deeper than 1 cm so that they may remain trapped in the ice at the higher temperatures of 100 K. If so, they may still be detectable by CAPS via sputtering of these molecules from the icy surface and their subsequent ionization in the vicinity of Dione [see Sittler et al., 2004b]. Finally, as previously noted, hydrogen peroxide may be a major molecule in the ice at Dione since water group ions are observed to dominate at all energies. Since ozone was detected at Dione and Rhea by HST [Noll et al., 1997], the presence of O_2 in the ice is highly likely. This is further supported by the detection of O_2^+ by the Cassini plasma instrument [Young et al., 2005; Sittler et al., 2005a].

It is important to note the measurements by Strazzulla et al. [2003], where they irradiated icy surfaces at temperatures between 16 K and 77 K with either 30 keV C^+ or N^+ ions. In the case of C^+ they did detect CO_2 and CO in the ice after irradiation. But for 30 keV N^+ ions incident on the ice, they only found nitrogen molecules if they had NH_3/CH_4 already in the ice. If the penetration depths and sputtering rates are such that the implanted N is removed efficiently or if a more volatile species such as N_2 formed and removed, the proposed chemistry, based on initially forming NO, might not occur. Therefore, the

nitrogen species due to implantation might be difficult to observe spectroscopically. However, in steady-state nitrogen species must be ejected into the gas-phase at a rate equivalent to the implantation rate. Therefore, such species will be observable by Cassini in the plasma.

9.0 SUMMARY AND CONCLUSIONS

In this paper we have made the case that Titan is the source of a large atomic nitrogen torus surrounding Saturn within the outer magnetosphere with L ~ 20 [Eviatar and Podolak, 1983; Eviatar et al., 1983; Barbosa, 1986; Ip, 1992; Smith et al., 2004] and that this cloud will be the source of keV pickup nitrogen ions, although dominated by keV O^+ ions as observed by Cassini [Crary et al., 2005; Hartle et al., 2006]. A subset of these keV nitrogen ions will then be transported into Saturn's inner magnetosphere where they will be energized by conserving the first and second adiabatic invariants. Johnson et al. [2005] have shown that charge exchange transport from the inner magnetosphere to the outer magnetosphere, may be an important source of oxygen within Saturn's outer magnetosphere. These will also be energized after ionization by inward diffusion. Enrichment processes [Sittler et al., 2006, manuscript in preparation] could enhance heavy ions relative to protons as they diffuse radially inward, could make heavy ions dominate the energetic ion population in the inner magnetosphere. The energetic nitrogen ions will then bombard the icy surfaces of the moons creating the complex nitrogen chemistry in their icy regolitha.

We reviewed the estimates of the source strength of hot neutral atoms from Titan. The primary uncertainty for estimating the source strength is the height of the ionopause and the access of magnetospheric plasma to the exobase or lower altitudes (Ip, 1992). Assuming an energy distribution with $f(E) = 1/(E+U)^2$ and U = 0.3 eV or a mono-energetic spectrum with ejection speeds ~ 1 km/s, we presented results of a Monte Carlo model of the nitrogen torus with uniform life time against ionization of $\tau_{N0} \sim 3 \times 10^8$ s. This model showed a neutral torus centered on Titan's orbit and extending into the inner magnetosphere with a thickness of $\pm$ 2 R_S near Titan. Using this source rate and the Voyager PLS observations, we estimated resident or transport time scales for the pickup ions to be ~ 7.4 hours. This is shorter than the lower limit estimated from radial diffusion coefficients as determined by Paonessa and Cheng (1986). The PLS data also indicates that within this torus the suprathermal ion component is confined to the equatorial plane so that $T_\perp / T_{ll} >> 1$. This is consistent with our calculations that give a neutral N torus thickness < 4 R_S.

We also looked into a solar wind source, with nitrogen getting ionized within the magnetosheath and then entering the magnetosphere similar to that for solar wind ions. A solar wind source could provide keV protons and alpha particles within Saturn's outer magnetosphere and be the source of energetic protons within Saturn's inner magnetosphere. In the case of entering N^+ ions, their pickup energies can be as high as 50-100 keV and with inward radial transport could achieve energies in excess of E ~ 1.6 MeV to 6.25 MeV. We determined that "solar wind" protons could be competitive relative to suprathermal N^+ ions from the Titan torus, but, parameter uncertainties are too

high to make a definitive statement. However, the PLS suprathermal ion measurements give a better fit assuming a heavy ion dominates over protons. In addition combining the PLS and LECP data we also get a better match assuming that heavy ions dominate the suprathermal fluxes. The paper by Maclennan et al. [1982] favors a proton composition within Saturn's outer magnetosphere for E > 30 keV. Finally, the re-analysis of the Voyager 1 plasma data at Titan by Sittler et al. [2004a, 2005b] showed that the keV component observed by PLS was in fact a heavy ion component such as O^+/N^+ because of finite gyro-radius effects. Finally, Cassini plasma observations have shown the keV component to be dominated by oxygen-methane ions [Crary et al., 2005; Hartle et al., 2006].

In a separate publication [Sittler et al., 2006, manuscript in preparation], we looked into ion losses due to satellite sweeping, impacts with dust-gas and precipitational losses due to wave-particle interactions. We found all losses to be comparable to transport time scales ~ 10 days. Furthermore, the MHD waves reported by Lepping et al. [2005] for 8.5 < L < 16.9 will tend to scatter the protons and make them isotropic, while transport time scales may be short enough so that $T_\perp / T_{ll} >> 1$ for the nitrogen ions as they are transported into the inner magnetosphere. In the case of N^+, with $T_\perp / T_{ll} >> 1$, the nitrogen ions will be confined near the equatorial plane and not be observable at high latitudes. When we consider the scattering time scales due to waves, L shell sweeping, observed particle losses reported by Armstrong et al. [1983] and the fact that Richardson et al. [1998] suggested that transport time scales could be longer between L ~ 7-12, transport time scales τ_R ~ 10 days seems highly probable at L ~ 8.5.

Eviatar et al. [1983] proposed that O^+ ions could charge exchange with the A-ring's hydrogen atmosphere just outside it's outer edge and produce a source of oxygen atoms within Saturn's outer magnetosphere (i.e., gravitationally bound to Saturn) with a source strength $S_O \sim 1.4 \times 10^{26}$ atoms/s. It was also noted that the charge exchange process inside of 4 R_S can occur by ion-molecule orbiting interactions which would recycle oxygen and other water products throughout the magnetosphere [Johnson et al., 1989; Johnson et al., 2005]. An oxygen torus that extends to the outer magnetosphere can produce a hot keV O^+ component similar to the hot keV N^+ component. Composition measurements within Saturn's magnetosphere by the CAPS instrument [Young et al., 2005; Crary et al., 2005; Sittler et al., 2005a; Hartle et al., 2006] and MIMI [Krimigis et al., 2005] have shown the O^+ and water group ions dominate throughout Saturn's magnetosphere with methane ions being an important contributor within the outer magnetosphere [Sittler et al., 2005a; Crary et al., 2005; Hartle et al., 2006]. Nitrogen ions evidently contribute only ~ 5% of the heavy ion component [Smith et al., 2005; Krimigis et al., 2005].

The PLS and LECP data during the Voyager 1 ring plane crossing of Dione's L shell are shown to be consistent with thermal protons and water group ions. The PLS suprathermal ion fluxes and the LECP data were best fit by a heavy ion like O^+ with 5% of N^+ [Young et al., 2005; Krimigis et al., 2005]. Using algorithms developed by Cooper et al. [2001] for the Galilean satellites, we computed the implantation rates and dosage rates for radiolysis as a function of depth for H^+, O^+ and N^+. Using highly uncertain G-values Delitsky and Lane [2004] concluded that nitrogen products would be a considerable

fraction of the surface, which is not likely. However, many of the species proposed have been observed in our laboratory as trapped molecules in an ice matrix: were N, NO, NO_2, HNO_3, N_2, and N_2O. These might be observable by the CAPS instrument during a targeted wake flyby of Dione as ions in ring distributions [see Sittler et al., 2004b]. CAPS detection of the freshly formed ions maybe more sensitive than IR absorbance spectra. Further, an exosphere surrounding Dione composed of the more volatile species might be observable by both VIMS NIR remote sensing measurements and CAPS *in situ* measurements.

10.0 ACKNOWLEDGEMENTS

Some of the work presented in this paper was performed at the Jet Propulsion Laboratory, California Institute of Technology under contract with NASA. At Goddard Space Flight Center, ECS, we acknowledge support from the CAPS Cassini Project. The work of REJ and HTS at Virginia was supported by the CAPS Cassini Instrument and by NASA's Planetary Atmosphere's Program. JFC also acknowledges support through Raytheon from NASA's Planetary Atmospheres Program and the Space Science Data Operations Office at NASA Goddard Space Flight Center.

REFERENCES

1. Armstrong, T.P., M.T. Paonessa, E.V. Bell II and S.M. Krimigis, Voyager observations of Saturnian ion and electron phase space densities, *J. Geophys. Res.*, **88**, 8893, 1983.
2. Barbosa, D.D., Medium energy electrons and heavy ions in Jupiter's magnetosphere: Effects of lower hybrid wave-particle interactions, *J. Geophys. Res.,* **91**, 5605-5615, 1986.
3. Barbosa, D.D. and A. Eviatar, Planetary fast neutral emission and effects on the solar wind: A cometary exosphere analog, *Astrophys. J.,* **310**, 927-936, 1986.
4. Barbosa, D.D., Titan's atomic nitrogen torus: Inferred properties and consequences for the Saturnian aurora, *Icarus,* **72**, 53, 1987.
5. Barbosa, D.D., Theory and observations of electromagnetic ion cyclotron waves in Saturn's inner magnetosphere, *J. Geophys. Res.*, **98**, 9345, 1993.
6. Book, D. L., Revised and enlarged collection of plasma physics formulas and data, *NRL Memo. Rep.*, **3332**, Naval Res. Lab., Washington D. C., 1977.
7. Brecht, S. H., J. G. Luhmann and D. J. Larson, Simulation of the Saturnian magnetospheric interaction with Titan, *J. Geophys. Res.*, **105**, 13,119-13,130, 2000.
8. Bridge, H.S., J.W. Belcher, R.J. Butler, A.J. Lazarus, A.M. Mavretic, J.D. Sullivan, G.L. Siscoe and V.M. Vasyliunas, The plasma experiemtn on the 1977 Voyager Mission, *Space Sci. Rev.,* **21**, 259, 1977.
9. Broadfoot, A. L., B.R. Sandel, D.E. Shemansky, J.B. Holberg, G.R. Smith, D.F. Strobel, J.C. McConnell, S. Kumar, D.M. Hunten, S.K. Atreya, T.M. Donahue, H.W. Moos, J.L. Bertaux, J.E. Blamont and R.B. Pomphrey, Extreme ultraviolet

observations from Voyager 1 encounter with Saturn, *Science,* **212**, 206-211, 1981.

10. Burch, J. L., J. Goldstein, T.W. Hill, D.T. Young, F.J. Crary, A.J. Coates, N. Andre, W.S. Kurth and E.C. Sittler, Jr., Properties of local plasma injections in Saturn's magnetosphere, *Geophys. Res. Lett.*, **32**, No. 14, L14S02, 10.1029/2005GL022611, 2005.
11. Carbary, J. F., S. M. Krimigis, and and W.-H. Ip, Energetic particle measurements of Saturn's satellites, *J. Geophys. Res*., **88(A11)**, 8947-8958, 1983.
12. Carlson, R. W., A tenuous carbon dioxide atmosphere on Jupiter's moon Callisto, *Science*, **283**, 820-821, 1999.
13. Connerney, J.E.P., M.H. Acuna and N.F. Ness, Currents in Saturn's magnetosphere, *J. Geophys. Res.,* **88**, 8779, 1983.
14. Cooper, J. F., Nuclear cascades in Saturn's rings:Cosmic ray albedo neutron decay and origins of trapped protons in the inner magnetosphere, *J. Geophys. Res.*, **88**, 3945-3954, 1983.
15. Cooper, J. F., E. C. Sittler, Jr., S. Maurice, B. Mauk, and R. S. Selesnick, Local time asymmetry of drift shells for energetic electrons in the middle magnetosphere of Saturn, *Adv. Sp. Res*., **21(11)**, 1479-1482, 1998.
16. Cooper, J. F., R. E. Johnson, B. H. Mauk, H. B. Garrett and N. Gehrels, Energetic ion and electron irradiation of the icy Galilean satellites, *Icarus*, **149**, 133-159, 2001.
17. Crary, F. J., D. T. Young, R. A. Baragiola, B. L. Barraclough, J. –J. Berthelier, M. Blanc, M. Bouhram, A. J. Coates, R. E. Hartle, T. W. Hill, R. E. Johnson, D. J. McComas, M. Michael, D. Reisenfeld, E. C. Sittler, H. T. Smith, J. T. Steinberg, K. Szego and M. Thomsen, Dynamics and composition of plasma at Titan, *Science*, submitted, 2005.
18. Cravens, T.E., C.N. Keller, and B. Ray, Photochemical sources of non-thermal neutrals for the exosphere of Titan, *Plant. Space Sci.,* **45**, 889, 1997.
19. Curtis, S.A., R.P. Lepping and E.C. Sittler Jr., The centrifugal flute instability and the generation of Saturnian kilometric radiation, *J. Geophys. Res.,* **91**, 10,989-10,994, 1986.
20. Delitsky, M. L. and A. L. Lane, Saturn's inner satellites: Ice chemistry and magnetospheric effects, *J. Geophys. Res.*, **107(E11)**, 5093, 2002.
21. Eviatar, A., R. L. McNutt, Jr., G.L. Siscoe and J.D. Sullivan, Heavy ions in the outer Kronian magnetosphere, *J. Geophys. Res.,* **88**, 823-831, 1983.
22. Eviatar, A. and M. Podolak, Titan's gas and plasma torus, *J. Geophys. Res.,* **88**, 833-840, 1983.
23. Goertz, C.K., Detached plasma in Saturn's turbulence layer, *Geophys. Res. Lett.*, **10**, 455, 1983.
24. Hartle, R.E., E.C. Sittler Jr., K. W. Ogilvie, J. D. Scudder, A.J. Lazarus and S. K. Atreya, Titan's ion exosphere observed from Voyager 1, *J. Geophys. Res.*, **87**, 1383, 1982.
25. Hartle, R. E., E. C. Sittler, Jr., F. M. Neubauer, R. E. Johnson, H. T. Smith, F. J. Crary, D. J. McComas, D. T. Young, A. J. Coates, D. Simpson, S. Bolton, D. Reisenfeld, K. Szego, J. J. Berthelier, A. Rymer, J. Vilppola, J. T. Steinberg, and N. Andre, Preliminary interpretation of Titan plasma interaction as observed by

the Cassini Plasma Spectrometer: Comparison with Voyager, *Geophys. Res. Lett.*, in press, 2006.
26. Hill, T.W., Corotation lag in Jupiter's magnetosphere: Comparison of observation and theory, *Science,* **207**, 301-302, 1980.
27. Hunten, D.M., Thermal and nonthermal escape mechanisms for terrestrial bodies, *Planet. Space Sci.,* **30**, 773, 1982.
28. Hunten, D.M., M.G. Tomasko, F.M. Flaser, R.E. Samuelson, D.E. Strobel, et al., Titan, in *Saturn*, eds. T. Gehrels and M.S. Mathews, Univ. of Arizona Press, 671, 1984.
29. Ip, W.-H., Titan's ionosphere, *Astrophys. J.,* **362**, 354, 1990.
30. Ip, W., -H., The nitrogen tori of Titan and Triton, *Adv. Space Res.*, **12**, (8)73, 1992.
31. Johnson, R.E., Plasma-induced sputtering of an atmosphere, *Space Science Reviews*, **69**, 215-253, 1994.
32. Johnson, R. E., Pospieszalska, M. K., Sieveka, E. M., Cheng, A. F., Lanzerotti, L. J., and Sittler, E. C., "The Neutral Cloud and Heavy Ion Inner Torus at Saturn," *Icarus,* **77,** 311-329, 1989.
33. Johnson, R.E., M. Liu and C. Tully, Collisional dissociation cross-sections for O + O_2, CO and N_2, O_2 + O_2, N + N_2, and N_2 + N_2, *Planetary and Space Science,* **50**, 123, 2002.
34. Johnson, R.E., R.W. Carlson, J.F. Cooper, C. Paranicas, M.H. Moore, and M.C. Wong, "Radiation Effects on the Surface of the Galilean Satellites", *In Jupiter-The Planet, Satellites and Magnetosphere*, Ed. F. Bagenal, T. Dowling, and W.B. McKinnon, *Cambridge University, Combridge* in press, 2004.
35. Johnson, R. E., M. Liu and E. C. Sittler Jr., Plasma-induced clearing and redistribution of material embedded in planetary magnetospheres, *Geophys. Res. Lett.*, **32**, L24201, doi:10.1029/2005GL024275, 2005.
36. Jurac, S., R. E. Johnson, and J. D. Richardson, Saturn's E ring and production of the neutral torus, *Icarus*, **149**, 384, 2001.
37. Jurac, S. and J. D. Richardson, A self-consistent model of plasma and neutrals at Saturn: Neutral cloud morphology, *J. Geophys. Res.*, **110**, A09220, doi:10.1029/2004JA010635, 2005.
38. Keller, C. N., T. E. Cravens and L. Gan, A model of the ionosphere of Titan, *J. Geophys. Res.*, **97**, 12,117, 1992.
39. Keller, C. N., V. G. Anicich and T. E. Cravens, Model of Titan's ionosphere with detailed hydrocarbon ion chemistry, *Planet. Space Sci.*, **46**, 1157-1174, 1998.
40. Krimigis, S.M., T.P. Armstrong, W.I. Axford, C.O. Bostrom, C.Y. Fan, G. Gloeckler and L.J. Lanzerotti, The low energy charged particle (LECP) experiment on the Voyager spacecraft, *Space Sci. Rev.*, **21**, 329, 1977.
41. Krimigis, S.M., J.F. Carbary, E.P. Keath, C.O. Bostrom, W.I. Axford, G. Gloeckler, L.J. Lanzerotti and T.P. Armstrong, Characteristics of hot plasma in the Jovian magnetosphere: Results from the Voyager spacecraft, *J. Geophys. Res.,* **86**, 8227, 1981.
42. Krimigis, S. M., J. F. Carbary, E. P. Keath, T. P. Armstrong, L. J. Lanzerotti, and G. Gloeckler, General characteristics of hot plasma and energetic particles in the

Saturnian magnetosphere: Results from the Voyager spacecraft, *J. Geophys. Res.*, **88**, 8871, 1983.
43. Krimigis, S. M., et al., Magnetospheric Imaging Instrument (MIMI) on the Cassini mission to Saturn/Titan, *Space Sci. Rev.*, **114**, 2004.
44. Krimigis, S. M. et al., The dynamic Saturn magnetosphere: First results from Cassini/MIMI, *Science*, **307**, 1270-1273, 2005.
45. Lammer, H. and S.J. Bauer, Atmospheric mass loss from Titan by sputtering, *Planet. Space Sci.,* **41**, 657, 1993.
46. Lazarus, A. J. and R. L. McNutt Jr., Low energy plasma ion observations in Saturn's magnetosphere, *J. Geophys. Res.*, **88**, 8831, 1983.
47. Lepping, R. P., E. C. Sittler, Jr., W. H. Mish, S. A. Curtis and B. T. Tsurutani, Analysis of waves in Saturn's magnetosphere: Voyager 1 observations, *J. Geophys. Res.*, **110**, A05201, doi:10.1029/2004JA010559, 2005.
48. Maclennan, C.G., L. J. Lanzerotti, S. M. Krimigis, R. P. Lepping and N. F. Ness, Effects of Titan on trapped particles in Saturn's magnetosphere, *J. Geophys. Res.*, **87**, 1411, 1982.
49. Mathie, R. A. and I. R. Mann, A correlation between extended intervals of ULF wave power and storm-time geosynchronous relativistic electron flux enhancements, *Geophys. Res. Lett.*, **27**, 3261-3264, 2000.
50. Maurice, S., E. C. Sittler Jr., J. F. Cooper, B. H. Mauk, M. Blanc, and R. S. Selesnick, Comprehensive analysis of electron observations at Saturn: Voyager 1 and 2, *J. Geophys. Res.*, **101**, 15211, 1996.
51. McDonough, T. R. and N. M. Brice, A Saturnian gas ring and recycling of Titan's atmosphere, *Icarus*, **20**, 136-145, 1973.
52. McIlwain, C. E., Substorm injection boundaries, In *Magnetospheric Physics*, edited by B. M. McCormac, D. Reidel, Hingham, Mass., 143, 1974.
53. McPherron, R. L., The role of substorms in the generation of magnetic storms, *Magnetic Storms*, Eds. B. T. Tsurutani, W. D. Gonzalez, Y. Kamide, J. K. Arballo, Geophysical Monograph 98, 131, 1997.
54. McPherron, R. L., D. N. Baker and L. F. Bargatze, Linear filters as a method of real time prediction of geomagnetic activity, Terra Scientific Publishing Co. (Tokyo), 85-92, 1986.
55. Michael, M., R.E. Johnson, M. Liu, J. G. Luhmann and V. I. Shematovich, Ejection of nitrogen from Titan's atmosphere by magnetospheric ions and pickup ions, *Icarus*, **175**, 263, 2005.
56. Moore, M. H. and R. L. Hudson, IR detection of H_2O_2 at 80 K in ion-irradiated laboratory ices relevant to Europa, *Icarus*, **145**, 282-288, 2000.
57. Morrison, D., T. V. Johnson, E. M. Shoemaker, L. A. Soderblom, P. Thomas, J. Veverka and B. A. Smith, Satellite of Saturn: Geological perspective, in *Saturn*, edited by T. Gehrels and M. S. Matthews, Univ. of Ariz. Press, Tucson, 1984.
58. Neubauer, F.M., D.A. Gurnett, J.D. Scudder, and R.E. Hartle, Titan's magnetospheric interaction, in *Saturn,* eds. T. Gehrels and M.S. Matthews, Univ. of Arizona Press, Tucson, 571, 1984.
59. Noll, K. S., T. Rousch, D. Cruikshank and R. E. Johnson, Detection of ozone on Saturn's satellites Dione and Rhea, *Nature*, **388**, 45, 1997.

60. Paonessa, M. T. and A. F. Cheng, A theory of satellite sweeping, *J. Geophys. Res.*, **90**, 3428-3434, 1985.
61. Paonessa, M. T. and A. F. Cheng, Limits on ion radial diffusion coefficients in Saturn's inner magnetosphere, *J. Geophys. Res.,* **91**, 1391-1396, 1986.
62. Paranicas, C. and A. F. Cheng, A model of satellite microsignatures for Saturn, Icarus, 125, 380, 1997.
63. Paranicas, C., A. F. Cheng, B. H. Mauk, E. P. Keath and S. M. Krimigis, Evidence of a source of energetic ions at Saturn, *J. Geophys. Res.*, **102**, 17,459-17,466, 1997.
64. Paranicas, C., R. B. Decker, B.H. Mauk, S.M. Krimigis, T.P. Armstrong and S. Jurac, *Geophys. Res. Lett.*, submitted, 2004.
65. Randall, B. A., Energetic electrons in the magnetosphere of Saturn, *J. Geophys. Res.*, **99**, 8771, 1994.
66. Richardson, J. D., Thermal ions at Saturn: Plasma parameters and implications, *J. Geophys. Res.*, **91**, 1381, 1986.
67. Richardson, J. D., A. Eviatar, M. A. McGrath, and V. M. Vasyliunas, OH in Saturn's magnetosphere: Observations and implications, *J. Geophys. Res.*, **103**, 20245, 1998.
68. Sandel, B.R. and A.L. Broadfoot, Morphology of Saturn's aurora, *Nature (London)*, **292**, 679-682, 1981.
69. Sandel, B.R., D.E. Shemansky, A.L. Broadfoot, J.B. Holberg, G.R. Smith, J.C. McConnell, D.F. Strobel, S.K. Atreya, T.M. Donahue, H.W. Moos, D.M. Hunten, R.B. Pomphrey and S. Linick, Extreme ultraviolet observations from the Voyager 2 encounter with Saturn, *Science,* **215**, 548-553, 1982.
70. Schultz, M. and L.J. Lanzerotti, Particle Diffusion in the Radiation Belts, *Physics and Chemistry in Space 7, Springer-Verlag*, 1974.
71. Shemansky, D. E. and D. T. Hall, The distribution of atomic hydrogen in the magnetosphere of Saturn, *J. Geophys. Res.*, **97**, 4143-4161, 1992.
72. Shemansky, D. E., P. Matherson, D. T. Hall, H.-Y. Hu and T. M. Tripp, Detection of the hydroxyl radical in the Saturn magnetosphere, *Nature*, **363**, 329-332, 1993.
73. Shemantovich, V.I., Kinetic modeling of suprathermal nitrogen atoms in the Titan's atmosphere: I. Sources, *Solar System Research,* **32**, 384, 1998.
74. Shemantovich, V.I., Kinetic modeling of suprathermal nitrogen atoms in the Titan's atmosphere: II. Escape flux due to dissociation processes, *Solar System Research,* **33**, 32, 1999.
75. Shematovich, V.I., C. Tully and R.E. Johnson, Suprathermal nitrogen atoms and molecules in Titan's corona, *Adv. Space Res.,* **27**, 1875-1880, 2001.
76. Shematovich, V. I., R. E. Johnson, M. Michael, and J. G. Luhmann, Nitrogen loss from Titan, *J. Geophys. Res.*, **108**, E085087, E6, 1-11, 2003.
77. Siscoe, G. L., N. F. Ness and C. M. Yeates, Substorms on Mercury?, *J. Geophys. Res.*, **80**, 4359, 1975.
78. Sittler, E. C., Jr., K. W. Ogilvie and J. D. Scudder, Survey of low energy plasma electrons in Saturn's magnetosphere: Voyager 1 and 2, *J. Geophys. Res.*, **88**, 8847, 1983.
79. Sittler, E. C., Jr., R. E. Hartle, A. F. Vinas, R. E. Johnson, H. T. Smith and I. Mueller-Wodard, Titan interaction with Saturn's magnetosphere: Mass loading

and ionopause location, Titan Symposium at ESTEC, J. P. Lebreton Editor, 2004a.

80. Sittler, E.C., Jr.,R.E. Johnson, S. Jurac, J.D. Richardson, M. McGrath ,F. Crary, D. Young and J.E. Nordholt, Pickup ions at Dione and Enceladus: Cassini Plasma Spectrometer Simulations, *J. Geophys. Res.,* **109**, A01214, 2004b.
81. Sittler, E. C., Jr., M. Thomsen, D. Chornay, M. D. Shappirio, D. Simpson, R. E. Johnson, H. T. Smith, A. J. Coates, A. M. Rymer, F. Crary, D. J. McComas, D. T. Young, D. Reisenfeld, M. Dougherty and N. Andre, Preliminary results on Saturn's inner plasmasphere as observed by Cassini: Comparison with Voyager, *Geophys. Res. Lett.*, **32**, L14S07, doi:10.1029/2005GL022653, 2005a.
82. Sittler, E. C., Jr., R. E. Hartle, A. F. Vinas, R. E. Johnson, H. T. Smith, and I. Mueller-Wodarg, Titan interaction with Saturn's magnetosphere: Voyager 1 results revisited, *J. Geophys. Res.*, **110**, A09302, doi:10.1029/2004JA010759, 2005b.
83. Sittler, E. C., Jr., et al., Energetic Particle Ion Source, Loss and Transport within Saturn's Magnetosphere: Heavy Ions versus Protons, *J. Geophys. Res.*, manuscript in preparation, 2006.
84. Slavin, J. A. and R. E. Holzer, The effect of erosion on the solar wind stand-off distance at Mercury, *J. Geophys. Res.*, **84**, 2076, 1979.
85. Smith, E. J., L. Davis Jr., D. E. Jones, P. J. Coleman, Jr., D. S. Colburn, P. Dyal and C. P. Sonett, Saturn's magnetosphere and its interaction with the solar wind, *J. Geophys. Res.*, **85**, 5655, 1980.
86. Smith, E.J. and B. T. Tsurutani, Saturn's magnetosphere: Observations of ion cyclotron waves near the Dione L shell, *J. Geophys. Res.*, **88**, 7831, 1983.
87. Smith, H. T., R. E. Johnson and V. Shemantovich, Titan's atomic and molecular nitrogen tori, *Geophys. Res. Lett.*, 2004GL020580, 2004.
88. Smith, H. T., M. Shappirio, E. C. Sittler, D. Reisenfeld, R. E. Johnson, R. A. Baragiola, F. J. Crary, D. J. McComas and D. T. Young, Discovery of nitrogen in Saturn's inner magnetosphere, *Geophys. Res. Lett.*, **32**, L14S03, doi:10.1029/2005GL022654, 2005.
89. Sonnerup, B. U. and K. D. Siebert, Theory of the low latitude boundary layer and its coupling to the ionosphere: A tutorial review, *Earth's Low-Latitude Boundary Layer*, Eds. P. T. Newell and T. Onsager, American Geophysical Union Press, **133**, 13-32, 2003.
90. Southward, D. J. and W. J. Hughes, Theory of hydrodynamic waves in the magnetosphere, *Space Sci. Rev.,* **35**, 301-366, 1983.

91. Stevenson, D.J., Volcanism and igneous processes in small icy satellites, *Nature*, **298**, 142, 1982.

92. Spencer, J. R., W. M. Calvin and M. J. Person, CCD spectra of the Galilean satellites: Molecular oxygen on Ganymede, *J. Geophys. Res.*, **100**, 19049-19056, 1995.

93. Strazzulla, G., G. Leto, O. Gomis and M. A. Satorre, Implantation of carbon and nitrogen ions in water ice, *Icarus*, **164**, 163-169, 2003.

94. Strobel, D.F. and D.E. Shemansky, EUV emission from Titan's upper atmosphere: Voyager 1 encounter, *J. Geophys. Res.*, **87**, 1361-1368, 1982.

95. Strobel, D.F., M.E. Summers and X. Zhu, Titan's upper atmosphere: Structure and ultraviolet emissions, *Icarus,* **100**, 512, 1992.
96. Thompson, W.R., et al., One-electron capture in collisions of 6-100 keV protons with oxygen atoms, *J. Phys. B: At. Mol. Opt. Phys.*, **29**, 725-732, 1996.
97. Tsurutani, B.T. and G.S. Lakhina, Some basic concepts of wave-particle interactions in collisionless plasmas, *Rev. of Geophys.*, **35**, 491, 1997.
98. Tsurutani, B.T., X.Y. Zhou, V.M. Vasyliunas, G. Haerendel, J.K. Arballo and G.S. Lakhina, Interplanetary shocks, magnetopause boundary layers and dayside auroras: The importance of a very small region, *Surveys in Geophysics*, **22**, 101, 2001.
99. Tsurutani, B.T., G.S. Lakhina, L. Zhang, J.S. Pickett and Y. Kasahara, ELF/VLF plasma waves in the Low Latitude Boundary Layer, *in Earth's Low Latitude Boundary Layer*, edited by P. Newell and T. Onsager, American Geophysical Union Press, **133**, 189, 2003.
100. Vasyliunas, V.M., Mathematical models of magnetospheric convection and its coupling to the ionosphere, In *Particles and Fields in the Magnetosphere*, ed. B. M. McCormac, D. Reidel, Dordrecht, Netherlands, 60-71, 1970.
101. Vasyliunas, V. M., Concepts of magnetospheric convection, In *The Magnetospheres of the Earth and Jupiter*, ed. V. Formisano, D. Reidel, Dordrecht, 179-188, 1975.
102. Vasyliunas, V.M. and G.L. Siscoe, On the flux and the energy spectrum of interstellar ions in the solar system, *J. Geophys. Res.*, **81**, 1247, 1976a.
103. Vasyliunas, V. M., An overview of magnetospheric dynamics, In *Magnetospheric Particle and Fields*, ed. B. M. McCormac, D. Reidel, Dordrecht, 99-110, 1976b.
104. Warwick, J.W., J.B. Pierce, D.R. Evans, T.D. Carr, J.J. Schauble, J.K. Alexander, M.L. Kaiser, M.D. Desch, M. Pedersen, A. Lecacheux, G. Daigne, A. Boischot and C.H. Barrow, Planetary radio astronomy observations from Voyager 1 near Saturn, *Science,* **212**, 239-243, 1981.
105. Young, D. T., et al., Cassini Plasma Spectrometer Investigation, *Space Sci. Rev.*, **114**, 1-112, 2004.
106. Young, D. T., et al., Composition and dynamics of plasma in Saturn's magnetosphere, *Science*, **307**, 1262, 2005.

Figure Captions

Figure 1. (a) A 2D Monte Carlo calculation of Titan's atomic nitrogen torus assuming a sputtered source with source strength of $S_N \sim 4.5x10^{25}$ N/s, an energy spectrum characteristic of sputtered neutrals, spectral parameter U ~ 0.3 eV and lifetime of atomic nitrogen within Saturn's magnetosphere of $\tau_{N0} \sim 3x10^8$ sec. (b) Same as (a), except monoenergetic lanching energy with speed ~ 1 km/s is used. See text for details.

Figure 2. Voyager 1 PLS plasma ion data observed within Titan's atomic neutral torus near the ring plane. A three-component Maxwellian spectrum was fit to the data where the presence of a heavy suprathermal component is clearly evident.

Figure 3. Voyager 2 PLS plasma ion data observed near Titan's L shell, but at high latitudes, well above the ring plane. Interference in sensor's A, B and C is present at the higher ion energies which makes interpretation of this data difficult. But, it is felt that the measurements in the D cup are of good quality and shows no evidence of a suprathermal component. This interpretation is based on a survey of such measurements within Saturn's outer magnetosphere where the Titan nitrogen torus is expected to reside.

Figure 4. A combined plot of Voyager 1 PLS and LECP ion data within the Titan torus during the spacecraft inbound pass of Saturn's magnetosphere. For the thermal ions we used H^+ and O^+, while the suprathermal component for PLS was assumed to be O^+/N^+. For the LECP data we assumed O^+/N^+. In the case of the ion data labeled as PLS, we have interpolated the intensities from 5 keV to 10 keV. We have also super-imposed the Voyager 1 and 2 electron data from PLS and LECP. The CRS (Cosmic Ray Detector System) fluxes in this outer region went undetected. We have combined the Voyager 1 and electron data, since the Voyager 1 LECP instrument had its gamma detectors turned off, while they were on for Voyager 2. The high energy electron data was less latitudinal dependent, but this is not the case for the thermal electrons (i.e., plasma centrifugally confined). The particle fluxes have been converted into intensities.

Figure 5. Voyager 1 PLS ion spectrum measured during the Dione ring plane crossing. A three-component Maxwellian fit was performed with H^+ and O^+ used for the thermal component and H^+ used for the suprathermal component. The presence of a suprathermal ion component is clearly evident. This fit shows that protons provide a poor fit to the suprathermal component. This is clearly evident in the D cup measurements.

Figure 6. The same as Figure 5, except $N^+(O^+)$ is now used instead of protons. Here, because of a Mach number effect, the fit is considerably improved. It is felt that by using a shell distribution we would get a better fit to the A, B and C sensors. But, this needs to be confirmed by more quantitative calculations where a shell distribution is assumed for the suprathermal component.

Figure 7. A combined plot of PLS and LECP ion data recorded during the Voyager 1 ring plane crossing at Dione's L shell. For PLS we have assumed H^+ and O^+ for the thermal

ions and O^+ for the suprathermal ions. For the LECP data we have assumed O^+/N^+ ions. In the case of the ion data labeled as PLS, we have interpolated the intensities from 5 keV to 10 keV. We have also super-imposed the Voyager 1 and 2 electron data from PLS, LECP and CRS (Cosmic Ray Detector System). We have done this since the Voyager 1 LECP instrument had its gamma detectors turned off, while they were on for Voyager 2. The high energy electron data was less latitudinal dependent, but this is not the case for the thermal electrons (i.e., plasma centrifugally confined). The particle data has been converted into intensities.

Figure 8. Using the data in Figure 7 and assuming O^+/N^+ ions for E > 10 keV, we have computed the ion implantation rates as a function of depth for H^+, O^+ and N^+ within the icy surface of the moon Dione. See text for details.

Figure 9. Similar to that done for Figure 8, we have computed the dosage time scales for radiolysis as a function of depth in the icy surface of Dione. This figure shows the time scales at which radiolytic chemistry can occur as a function of depth in the ice.

Figure 10. Infrared spectrum of $H_2O + N_2 + O_2$ (3:1:1) at 20 K before and after irradiation with 0.8 MeV protons. The spectrum before irradiation shows small absorption features due to the forbidden transitions of both N_2 and O_2. After irradiation to a dose of ~ 4 eV (16 amu molecule)$^{-1}$, product molecules NO, NO_2, N_2O, O_3, and H_2O_2 are easily identified.

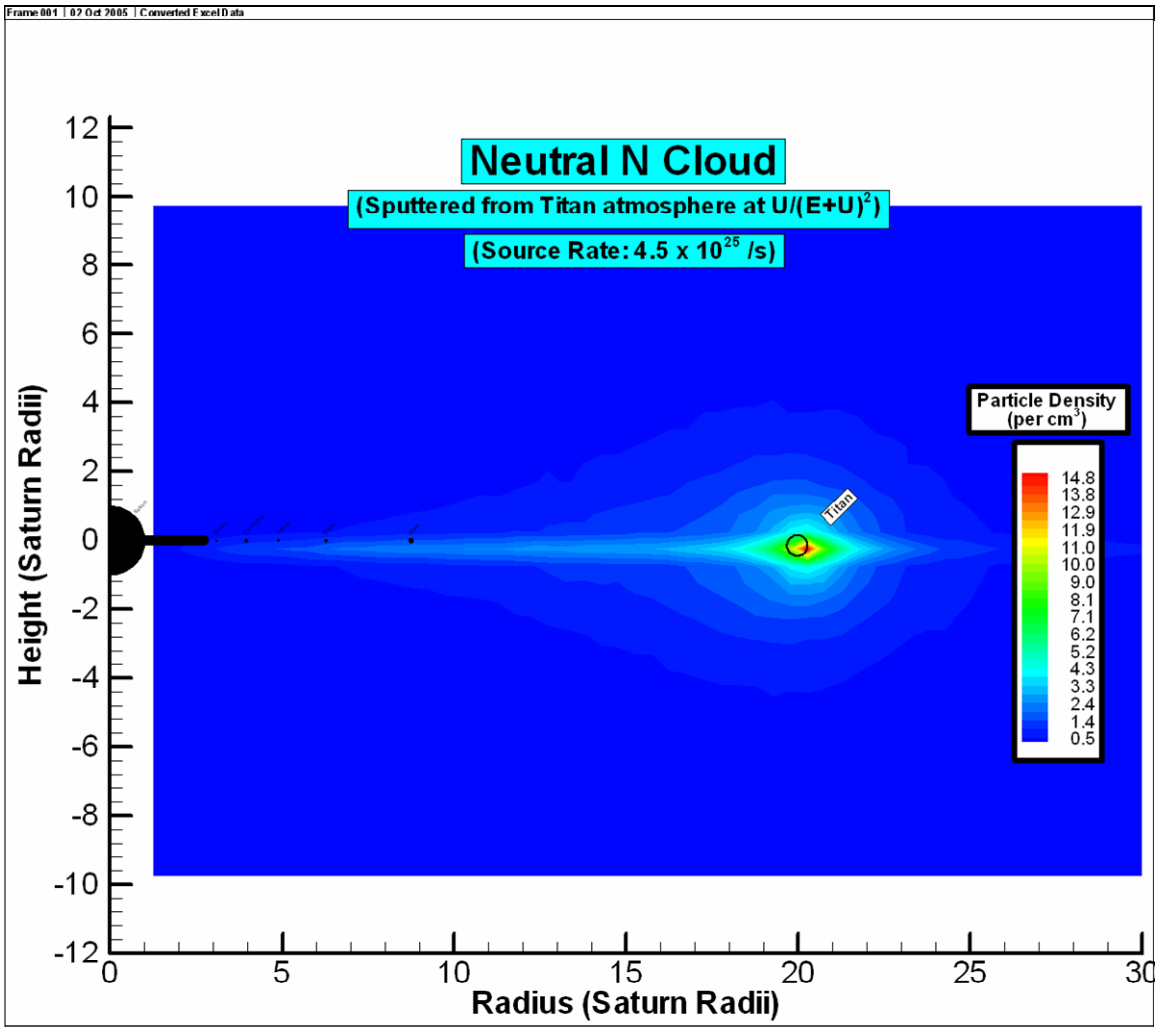
Frame 001 | 02 Oct 2005 | Converted Excel Data
Neutral N Cloud
(Sputtered from Titan atmosphere at U/(E+U)^2)
(Source Rate: 4.5 x 10^{25} /s)
Particle Density (per cm^3)
14.8
13.8
12.9
11.9
11.0
10.0
9.0
8.1
7.1
6.2
5.2
4.3
3.3
2.4
1.4
0.5
Titan
Height (Saturn Radii)
12
10
8
6
4
2
0
-2
-4
-6
-8
-10
-12
0
5
10
15
20
25
30
Radius (Saturn Radii)

Figure 1a.

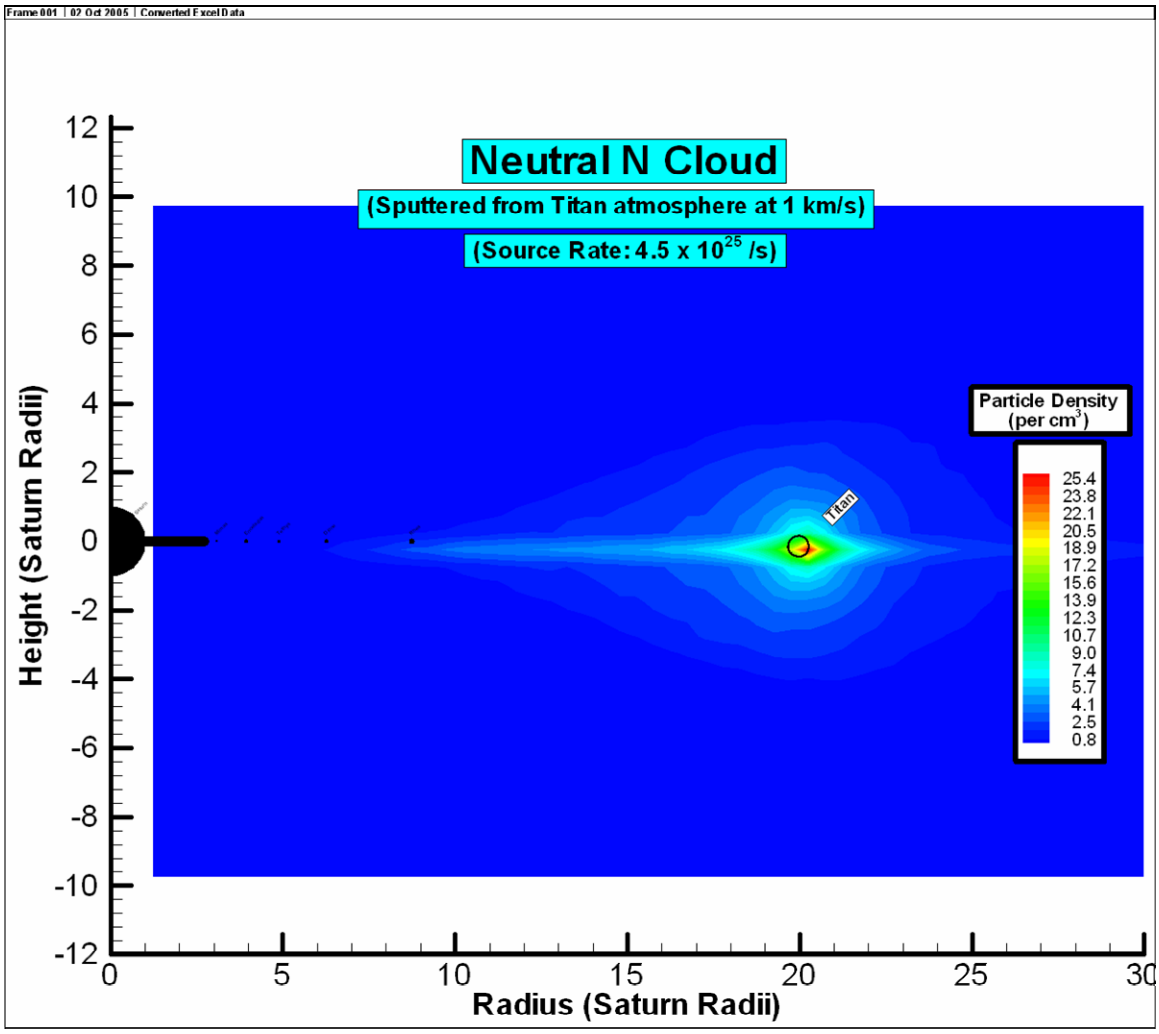
Frame 001 | 02 Oct 2005 | Converted Excel Data
Neutral N Cloud
(Sputtered from Titan atmosphere at 1 km/s)
(Source Rate: 4.5 x 10^25 /s)
Particle Density (per cm^3)
25.4
23.8
22.1
20.5
18.9
17.2
15.6
13.9
12.3
10.7
9.0
7.4
5.7
4.1
2.5
0.8
Titan
Height (Saturn Radii)
Radius (Saturn Radii)
12
10
8
6
4
2
0
-2
-4
-6
-8
-10
-12
0
5
10
15
20
25
30

Figure 1b.

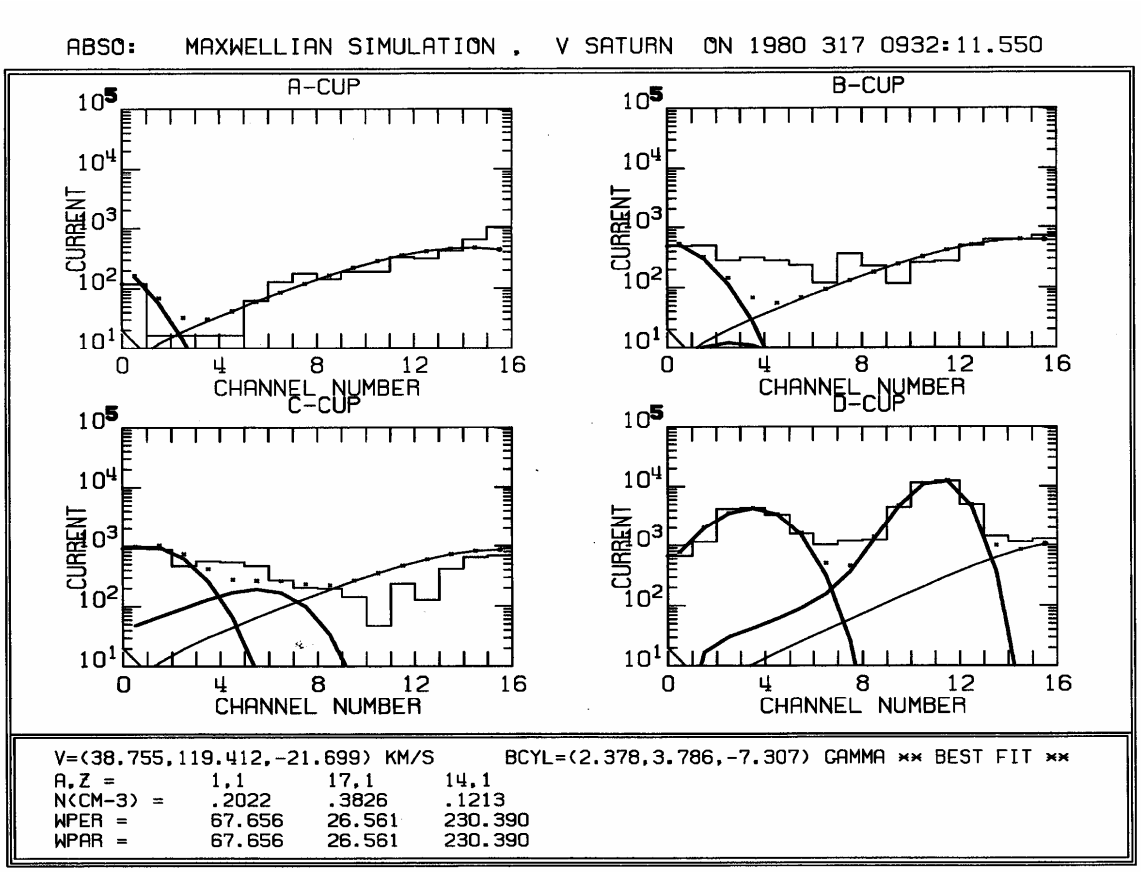
ABSO: MAXWELLIAN SIMULATION , V SATURN ON 1980 317 0932:11.550
A-CUP
B-CUP
C-CUP
D-CUP
CURRENT
CHANNEL NUMBER
V=(38.755,119.412,-21.699) KM/S
BCYL=(2.378,3.786,-7.307) GAMMA ** BEST FIT **
A,Z = 1,1 17,1 14,1
N(CM-3) = .2022 .3826 .1213
WPER = 67.656 26.561 230.390
WPAR = 67.656 26.561 230.390

Figure 2.

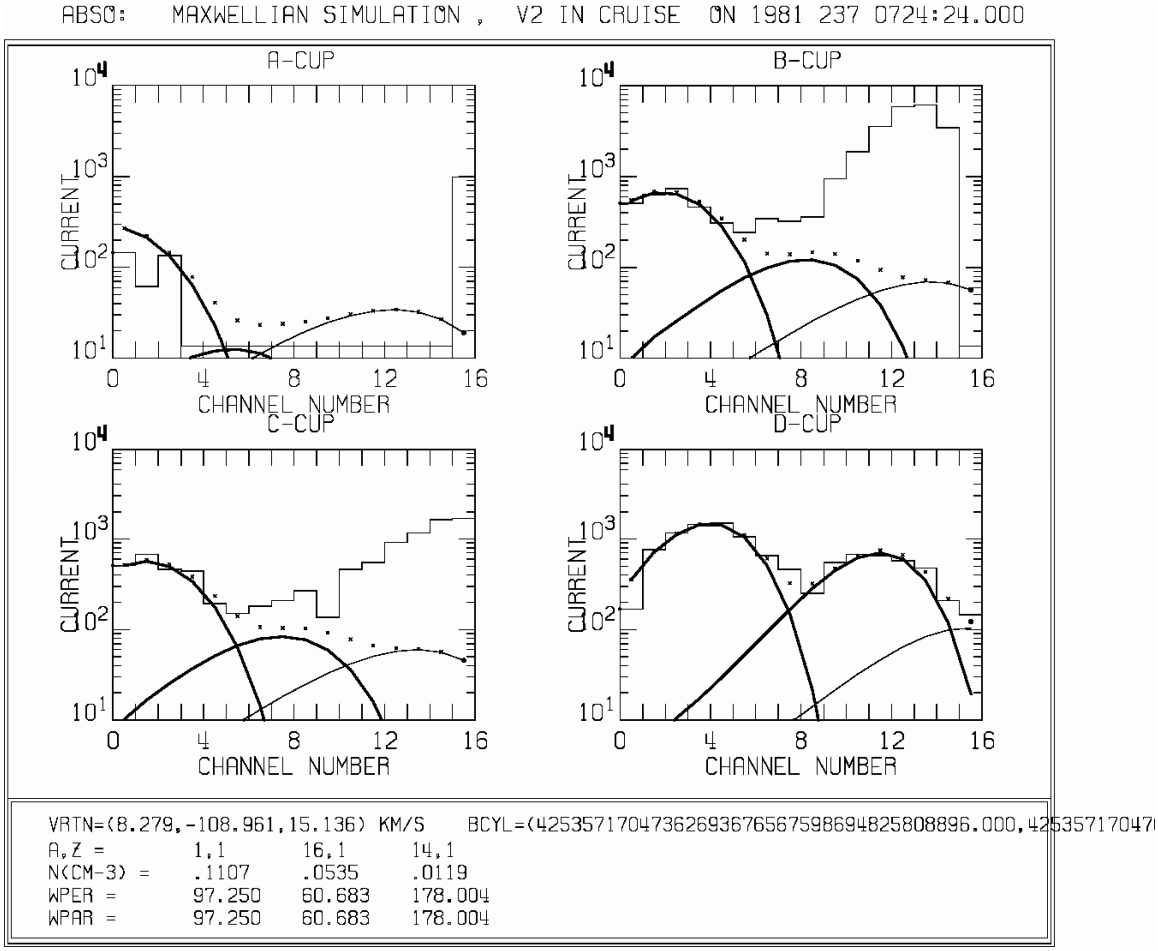
ABSO: MAXWELLIAN SIMULATION , V2 IN CRUISE ON 1981 237 0724:24.000
A-CUP
B-CUP
C-CUP
D-CUP
CURRENT
CHANNEL NUMBER
VRTN=(8.279,-108.961,15.136) KM/S
BCYL=(42535717047362693676567598694825808896.000,42535717047
A,Z = 1,1 16,1 14,1
N(CM-3) = .1107 .0535 .0119
WPER = 97.250 60.683 178.004
WPAR = 97.250 60.683 178.004

Figure 3.

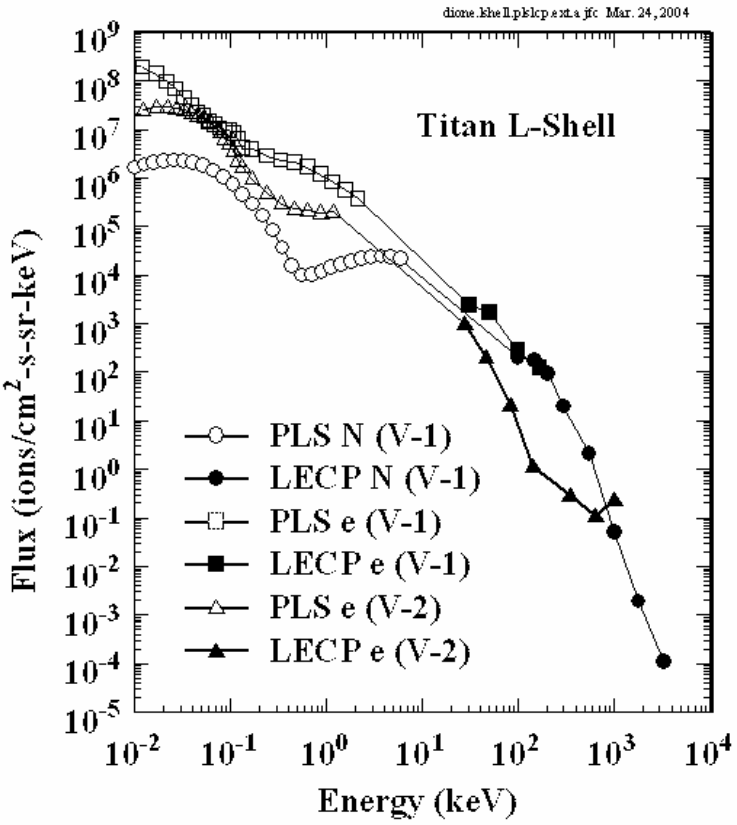
dione.khell.plslcp.extra.jfc Mar. 24, 2004
Titan L-Shell
PLS N (V-1)
LECP N (V-1)
PLS e (V-1)
LECP e (V-1)
PLS e (V-2)
LECP e (V-2)
Flux (ions/cm^2-s-sr-keV)
Energy (keV)

Figure 4.

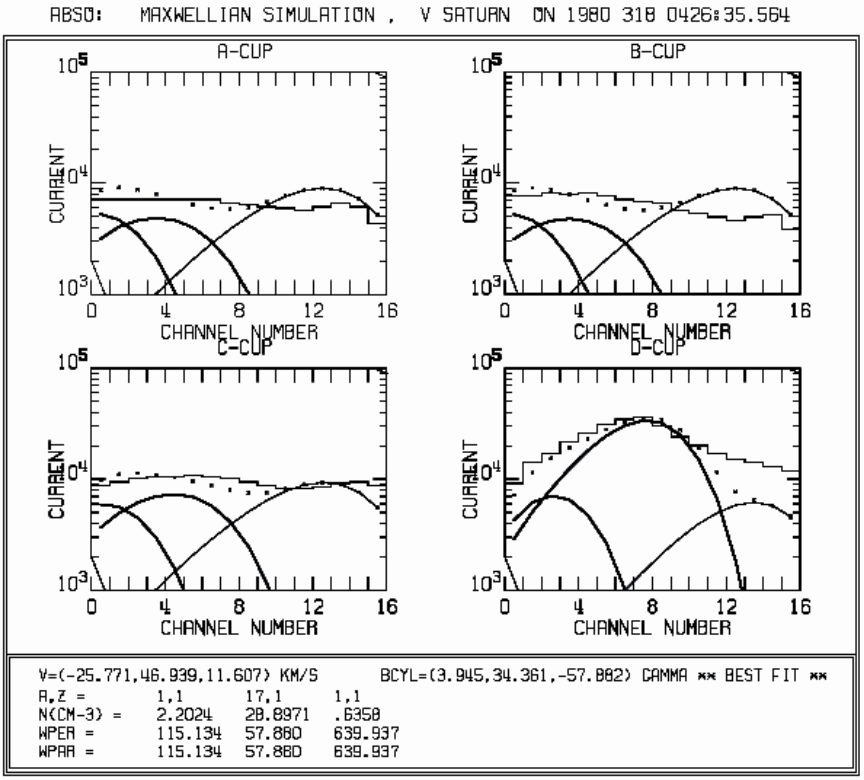
ABSO: MAXWELLIAN SIMULATION , V SATURN ON 1980 318 0426:35.564
A-CUP
B-CUP
C-CUP
D-CUP
CURRENT
CHANNEL NUMBER
V=(-25.771,46.939,11.607) KM/S
BCYL=(3.945,34.361,-57.882) GAMMA ** BEST FIT **
A,Z = 1,1 17,1 1,1
N(CM-3) = 2.2024 28.8971 .6358
WPER = 115.134 57.880 639.937
WPAR = 115.134 57.880 639.937

Figure 5.

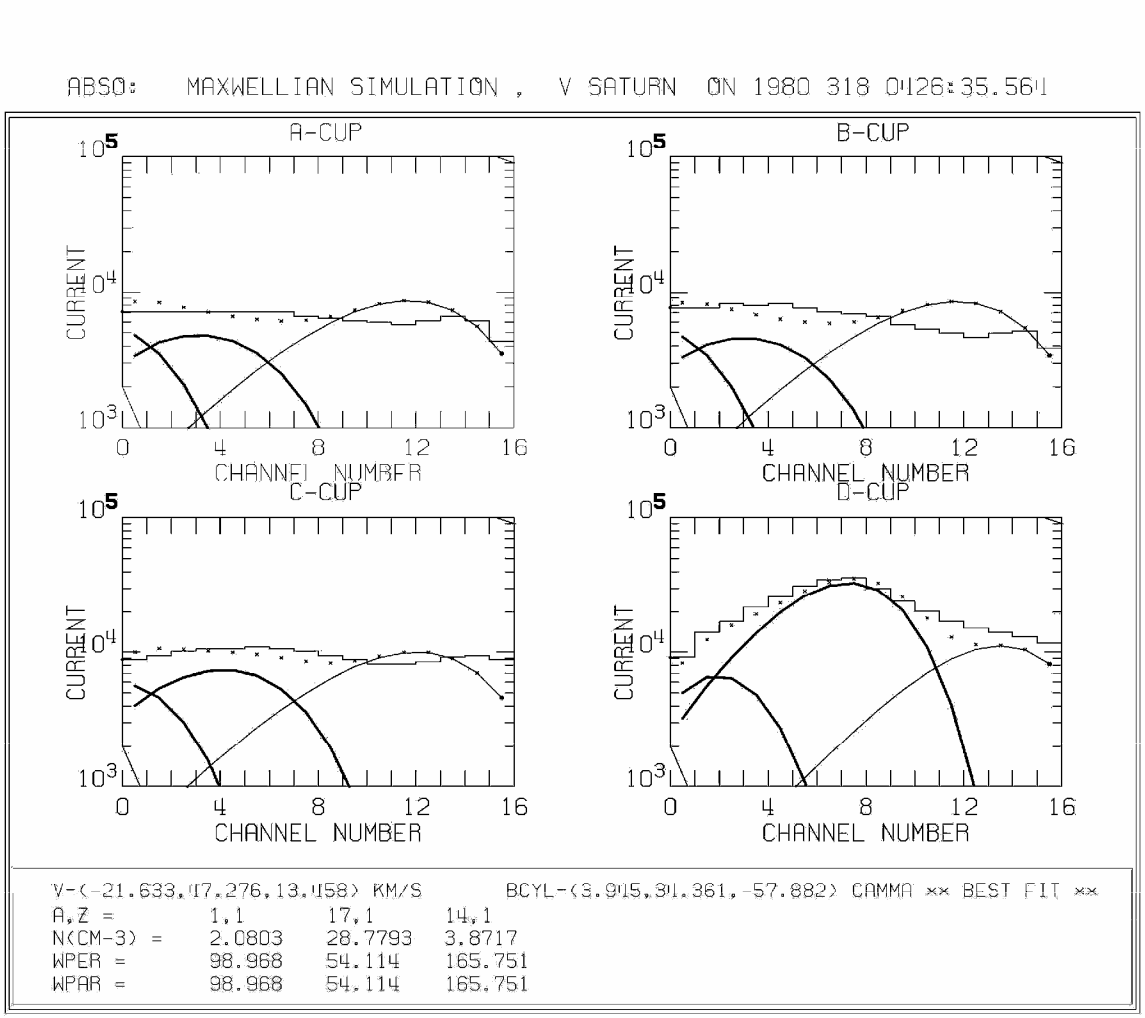
ABSO: MAXWELLIAN SIMULATION , V SATURN ON 1980 318 0:26:35.561
A-CUP
B-CUP
C-CUP
D-CUP
CURRENT
CHANNEL NUMBER
V-(-21.633,-7.276,13.458) KM/S
BCYL-(3.915,-91.361,-57.882) GAMMA ** BEST FIT **
A,Z = 1,1 17,1 14,1
N(CM-3) = 2.0803 28.7793 3.8717
WPER = 98.968 54.114 165.751
WPAR = 98.968 54.114 165.751

Figure 6.

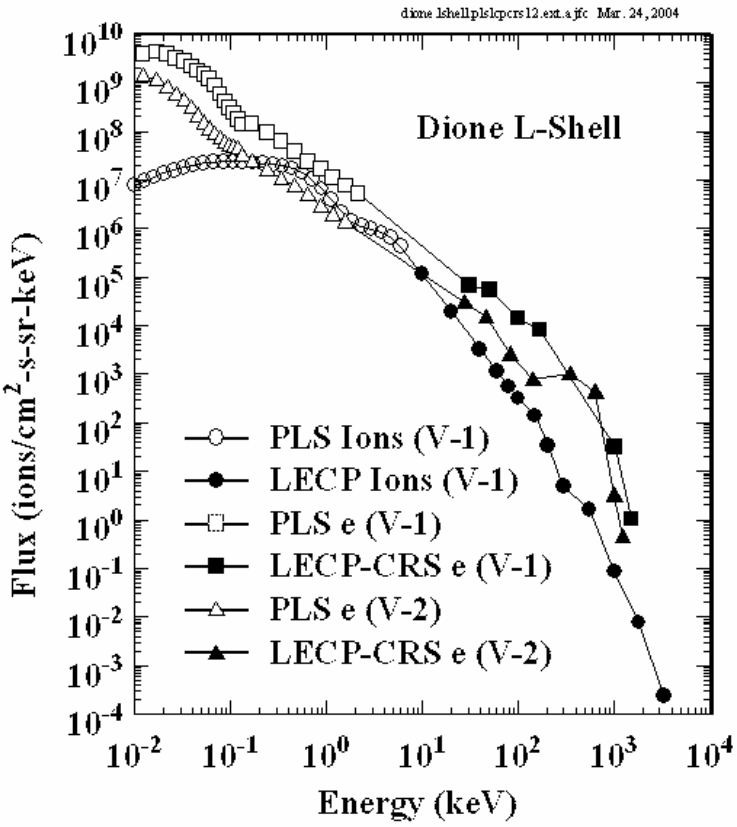
dione lshellplslcpcrs12.ext.a.jfc Mar. 24, 2004
Dione L-Shell
PLS Ions (V-1)
LECP Ions (V-1)
PLS e (V-1)
LECP-CRS e (V-1)
PLS e (V-2)
LECP-CRS e (V-2)
Flux (ions/cm^2-s-sr-keV)
Energy (keV)
10^{10}
10^{9}
10^{8}
10^{7}
10^{6}
10^{5}
10^{4}
10^{3}
10^{2}
10^{1}
10^{0}
10^{-1}
10^{-2}
10^{-3}
10^{-4}
10^{-2}
10^{-1}
10^{0}
10^{1}
10^{2}
10^{3}
10^{4}

Figure 7.

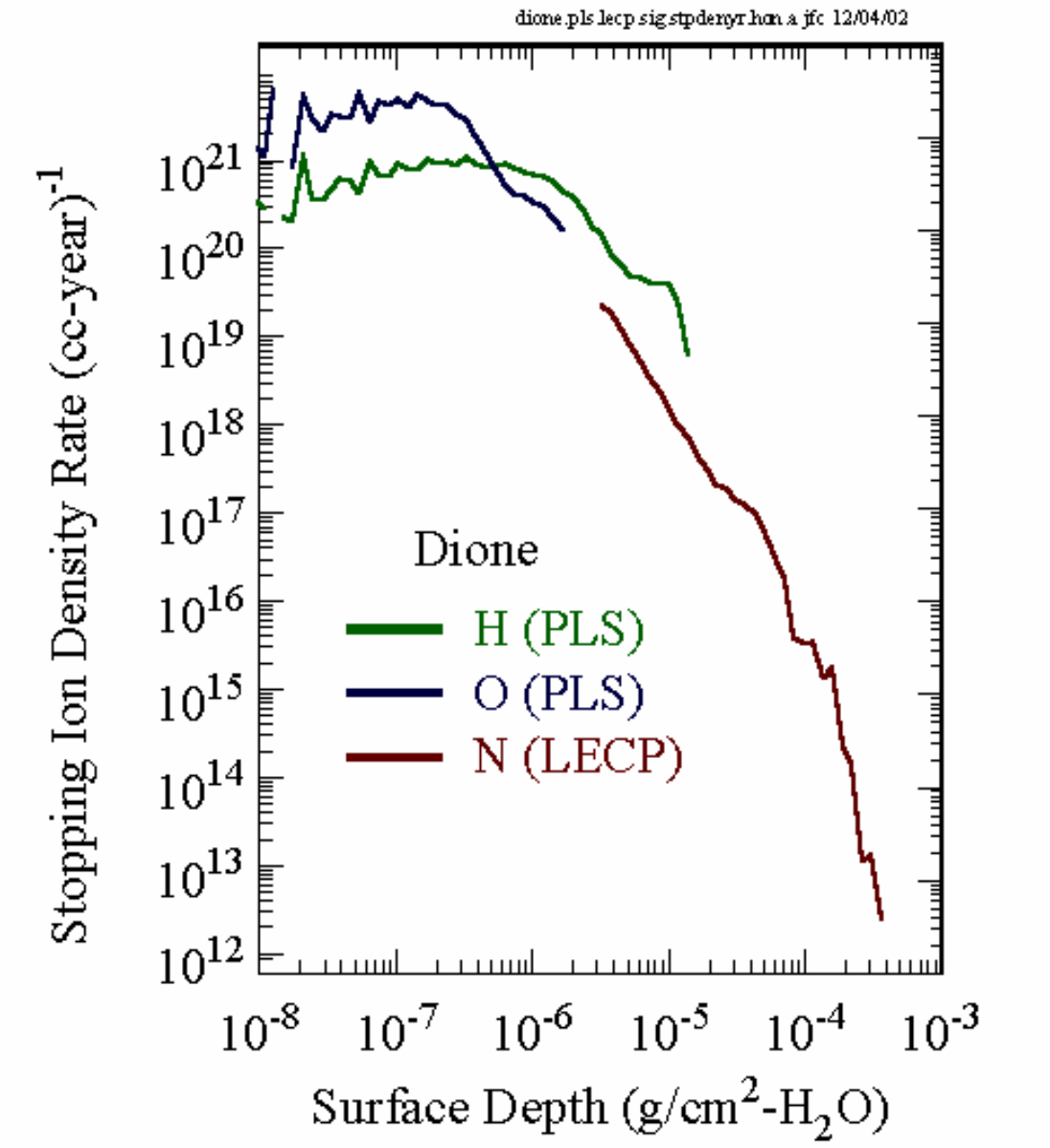
dione.pls lecp sig stpdenyr hon a jfc 12/04/02
Stopping Ion Density Rate (cc-year)$^{-1}$
10^{21}
10^{20}
10^{19}
10^{18}
10^{17}
10^{16}
10^{15}
10^{14}
10^{13}
10^{12}
Dione
H (PLS)
O (PLS)
N (LECP)
10^{-8}
10^{-7}
10^{-6}
10^{-5}
10^{-4}
10^{-3}
Surface Depth (g/cm^2-H_2O)

Figure 8.

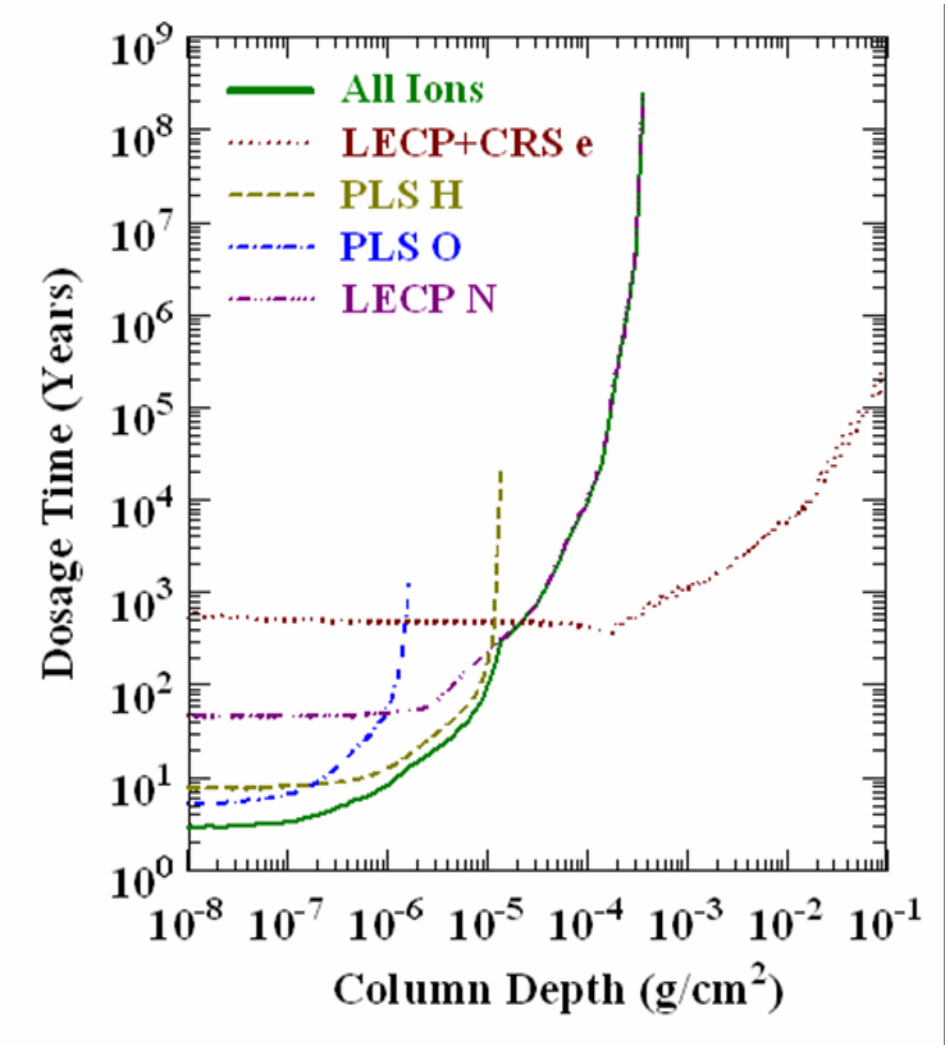
All Ions
LECP+CRS e
PLS H
PLS O
LECP N
Dosage Time (Years)
Column Depth (g/cm²)
10⁹
10⁸
10⁷
10⁶
10⁵
10⁴
10³
10²
10¹
10⁰
10⁻⁸ 10⁻⁷ 10⁻⁶ 10⁻⁵ 10⁻⁴ 10⁻³ 10⁻² 10⁻¹

Figure 9.

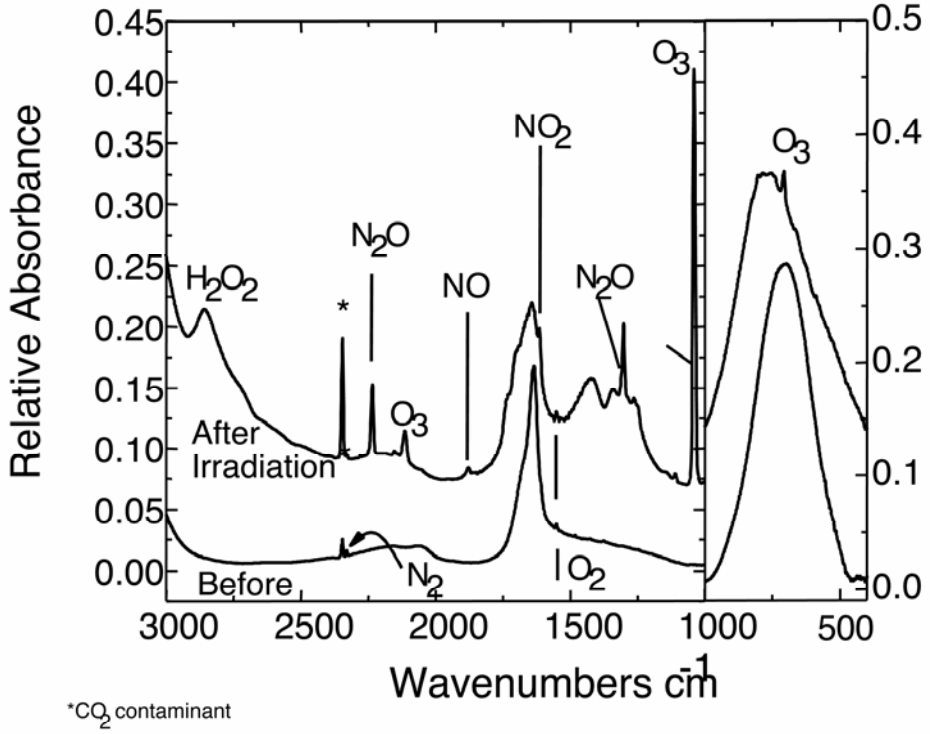
Relative Absorbance
0.45
0.40
0.35
0.30
0.25
0.20
0.15
0.10
0.05
0.00
0.5
0.4
0.3
0.2
0.1
0.0
3000
2500
2000
1500
1000
500
Wavenumbers cm -1
H2O2
*
N2O
O3
NO
NO2
N2O
O3
O3
After
Irradiation
Before
N2
O2
*CO2 contaminant

Figure 10.